



Contents lists available at ScienceDirect

## Arabian Journal of Chemistry

journal homepage: [www.ksu.edu.sa](http://www.ksu.edu.sa)

Original article



# Cytotoxic diterpenoids from the roots of *Euphorbia jolkinii* Boiss against human pancreatic cancer SW1990 cells by regulating the expressions of Bcl-2, Bax, and Caspase-3 proteins

Xinglong Chen<sup>a,1</sup>, Hongbo Zhu<sup>a,1</sup>, Haiying Zhang<sup>a,1</sup>, Tang Zhou<sup>a</sup>, Xingxi Li<sup>a</sup>, Bo Hou<sup>a</sup>, Weiyuan Hu<sup>b,\*</sup>, Rongping Zhang<sup>a,\*</sup>

<sup>a</sup> School of Chinese Materia Medica & Yunnan Key Laboratory of Southern Medicine Utilization, Yunnan University of Chinese Medicine, Kunming 650500, PR China

<sup>b</sup> School of Pharmaceutical Science & Yunnan Key Laboratory of Pharmacology for Natural Products, Kunming Medical University, Kunming 650500, PR China

## ARTICLE INFO

## Keywords:

*Euphorbia jolkinii* Boiss  
Diterpenoids  
SW1990 cells  
Cytotoxicity  
Bcl-2

## ABSTRACT

Sixteen undescribed diterpenoids were identified from *Euphorbia jolkinii* Boiss, a widespread invasive plant in the grassland ecosystem of subalpine meadows in southwest China, through a combination of spectroscopic data analysis. These included two casbane diterpenoids (1 and 2), two *ent*-atisane diterpenoids (3 and 4), and twelve *ent*-isopimarane diterpenoids (5–16). All isolates were evaluated the cytotoxicity on pancreatic cancer SW1990 cells in which compounds 1 and 9 exhibited obvious bioactivities against the tumor cells with the IC<sub>50</sub> values of 26.50 ± 6.36 and 21.09 ± 5.98 μM respectively. Moreover, compounds 1 and 9 were found to promote the pre-apoptosis of SW1990 cells and regulate the expressions of Bcl-2, Bax, and Caspase-3 proteins to display anti-tumor abilities. Compounds 1 and 9 were subjected to Bcl-2 protein *via* molecular docking to reveal their anti-tumor mechanism further. The druggability prediction showed that they possessed good drug properties with development and utilization scenarios.

## 1. Introduction

Grassland ecosystem is an indispensable part of terrestrial ecosystem and an important support for human agricultural production (Guo et al., 2019). A large area of subalpine meadows is distributed in southwest China, which plays an important role in the development of local agriculture (Yang et al., 2019). However, the degradation problems of subalpine meadows in southwest China have occurred due to invasive plants (Feng et al., 2017). *Euphorbia jolkinii* Boiss, one of the widely distributed invasive plants in this area, is a perennial poisonous plant of Euphorbiaceae family with developing root system, strong cold resistance, drought resistance, and nutrient competition ability (Pharmacopoeia of P.R. China, 1997; Zhao et al., 2012). In recent years, it has been spreading in the degraded alpine meadow, resulting in the disappearances of the excellent herbaceous grasses and the degradations of grasslands which seriously affects the sustainable development of local agriculture and the protection of biodiversity (Niu et al., 2024; Li et al., 2021). Therefore, the preventions and utilizations of *E. jolkinii* have been become a hot research area.

Pancreatic cancer is one of the most common and highly malignant tumors in digestive system. Its morbidity and mortality are increasing which seriously threatens human health (Siegel et al., 2024; Siegel et al., 2023). Pancreatic cancer is easy to be misdiagnosed due to its hidden onset and the lack of specific manifestations in the early stage (Garg and Chari, 2020; Gupta et al., 2020). Once patients are diagnosed, they are in the advanced stage and difficult to undergo surgical treatment (Neoptolemos et al., 2018; Kunovaky et al., 2018). Thus, chemotherapy is often the preferred treatment strategy for patients with pancreatic cancer. However, the treatment effect of the existing drugs on pancreatic cancer is not good and the prognosis is poor which suggests that there is an urgent need to develop new drugs for the treatment of pancreatic cancer. Natural products have continually contributed with the treatment of pancreatic cancer by influencing the proteins associated with apoptosis such as Bcl-2, Bax, and Caspase-3 proteins. Piperine induced the apoptosis of pancreatic cancer cells through the regulation of Caspase-3, Bax, and Bcl-2 proteins (Zhong et al., 2020). The combination of melatonin and gemcitabine could down-regulate the expression of Bcl-2 protein and up-regulate the expression of Bax protein in human

\* Corresponding authors.

E-mail addresses: [huweiyuan2004@163.com](mailto:huweiyuan2004@163.com) (W. Hu), [zhrpkm@163.com](mailto:zhrpkm@163.com) (R. Zhang).

<sup>1</sup> These authors contributed equally to this work.

<https://doi.org/10.1016/j.arabjc.2024.106012>

Received 22 July 2024; Accepted 2 October 2024

Available online 6 October 2024

1878-5352/© 2024 The Author(s). Published by Elsevier B.V. on behalf of King Saud University. This is an open access article under the CC BY-NC-ND license (<http://creativecommons.org/licenses/by-nc-nd/4.0/>).

pancreatic cancer SW1990 cells to promote the apoptosis and necrosis of pancreatic cancer cells (Xu et al., 2013). The extracts of *Armeniaca vulgaris* Lam. seeds accelerated the apoptosis of human pancreatic cancer cells by up-regulating the ratios of Bax/Bcl-2 and Caspase-3 expressions (Aamazadeh et al., 2020).

Diterpenoids are the characteristic secondary metabolites of *E. jolkinii* roots from which *ent*-atisane diterpenoids, *ent*-isopimarane diterpenoids, and *ent*-abietane diterpenoids have been reported (Huang et al., 2014; He et al., 2008). Jolkinolide B, the main abietane diterpenoid obtained from *E. jolkinii* roots, presented obvious anti-tumor abilities to inhibit the growth of human chronic myeloid leukemia K562, prostate cancer cells LNCaP, and human breast cancer cells MCF-7 (Liu et al., 2002; Luo and Wang, 2006; Xu et al., 2013). But the cytotoxic effects of the diterpenoids from *E. jolkinii* roots on pancreatic cancer cells were unclear yet. Our research group has long been committed to discovery cytotoxic diterpenoids against pancreatic cancer cells. We have found that the diterpenoids isolated from *Tripterygium hypoglaucum* could kill the pancreatic cancer SW1990 cells by increasing the expression of Bax protein (Chen et al., 2022) which suggested us that diterpenoids were important sources to develop anti-pancreatic cancer drugs. Thus, it was possible to find cytotoxic diterpenoids against pancreatic cancer cells from *E. jolkinii* that promoted the utilization of *E. jolkinii*.

In this paper, the cytotoxic diterpenoids against pancreatic cancer cells from *E. jolkinii* roots were studied. As a result, sixteen undescribed diterpenoids were identified by a combination of spectroscopic data analysis and quantum-chemical electronic circular dichroism (ECD) calculations including two casbane diterpenoids, two *ent*-atisane diterpenoids, and twelve *ent*-isopimarane diterpenoids (Fig. 1). They were all evaluated the cytotoxicity on pancreatic cancer SW1990 cells in which compounds 1 and 9 exhibited obvious bioactivities against the tumor cells. 1 and 9 could regulate the expressions of apoptosis proteins, such as Bcl-2, Bax, and Caspase-3 proteins to display anti-tumor abilities. And we also evaluated their effects on the growth cycle of tumor cells and subjected them to the target protein *via* molecular docking to reveal their anti-tumor mechanism and drug properties. Herein, we reported the isolation, structural illumination, and cytotoxicity on pancreatic

cancer SW1990 cells of these diterpenoids from *E. jolkinii* roots.

## 2. Materials and methods

### 2.1. General experimental procedures

The high-resolution mass spectra were detected on LC-MS-IT-TOF (Shimadzu, Japan) and Agilent LC-MS-Q-TOF G6530 (Agilent Technologies, Santa Clara, USA). NMR data were conducted with a Bruker Advance III-600 spectrometer (Bruker, Massachusetts, USA) using tetramethylsilane (TMS) as an internal standard. The ultraviolet (UV) spectra were measured on a UV-2401 UV spectrometer (Shimadzu, Kyoto, Japan) and the electronic circular dichroism (ECD) spectra were recorded using a Chirascan instrument (Applied Photophysics, Surrey, UK). Infrared (IR) spectra were performed using KBr lithography on a NICOLET iS10 infrared spectrometer (Thermo Fisher Scientific Inc, Massachusetts, USA). Optical rotation data (ORD) were collected with Jasco model 1020 polarimeter (Horiba, Tokyo, Japan). The LC-52 system (Beijing Saipuruisi Technology Co., Ltd., Beijing, China) was employed for high-performance liquid chromatography (HPLC) purifications with a ReproSil-Pur 120 CN column (10 × 250 mm, 5 μm). Silica gel (200–300 mesh, Qingdao Makall group Co. Ltd., Qingdao, China), Sephadex LH-20 (20–50 μm, Amersham Bioscience, Sweden), MCI gel CHP 20P (Mitsubishi Chemical Corporation, Tokyo, Japan), and Rp-C18 column (40–70 μm, Mitsubishi Chemical Corporation, Tokyo, Japan), and thin-layer chromatography plate (GF254, 200 × 200 mm, Liyan Technology Co., Ltd., Kunming, China) were employed for the isolations. The thin layer chromatography (TLC) plate was sprayed with a 10 % H<sub>2</sub>SO<sub>4</sub>-EtOH (v/v) solution as a chromogenic agent. Microplate reader (HBS-1096B, DeTie, Nanjing, China) and thermostatic cell incubator (Thermo Forma 3310, Thermo Fisher Scientific Inc, Massachusetts, USA) were used. Fluorescein FITC-labelled Annexin-V, Propidium iodide (PI) and CCK-8 kit were obtained from BD Pharmingen, San Diego, USA. Paclitaxel (HPLC ≥ 98 %) was purchased from Liyan Technology Co., Ltd., Kunming, China. Primary antibodies against Bcl-2 (ab194583, abcam), Bax (ab32503, abcam), Caspase-3 (ab184787, abcam), β-actin (ab8226, abcam) were purchased from Abcam Co.

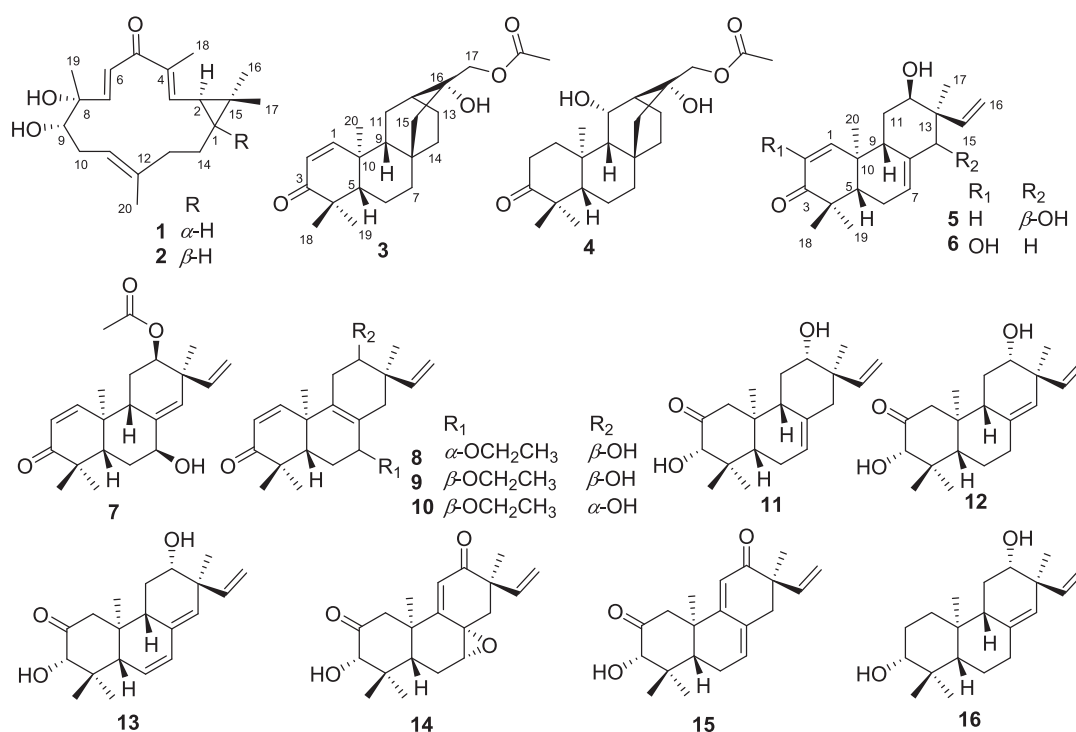


Fig. 1. The chemical structures of compounds 1–16.

Ltd., Cambridge, UK. Human pancreatic cancer cells (SW1990) were obtained from the Kunming Cell Bank of the Typical Culture Preservation Committee of the Chinese Academy of Sciences.

## 2.2. Plant materials

The roots of *Euphorbia jolkini* Boiss were collected in Shangri-la county, Yunnan province, in August 2020 and authenticated by Prof. Lu Lu (Kunming Medical University). A voucher specimen (No. 2020-0812) was deposited in Yunnan Key Laboratory of Southern Medicine Utilization.

## 2.3. Extraction and isolation

30.0 Kg of *E. jolkini* roots were smashed and extracted with MeOH (3 × 150 L) for three times at room temperature. The combined methanol extracts were suspended in H<sub>2</sub>O and extracted with ethyl acetate to obtain the EtOAc part (1.5 kg). Then the EtOAc fraction was fractionated by D101 macroporous resin column using an EtOH-H<sub>2</sub>O gradient system (30:70, 50:50, 70:30, and 90:10, v/v) to afford four fractions (Fr.1–Fr.4).

Fr.3 (480 g) was subjected to MCI column chromatography (CC) and eluted with a gradient system of MeOH-H<sub>2</sub>O (50:50–90:10, v/v) to give four fractions, Fr.3-1–Fr.3-4. Fr.3-2 (95.6 g) was subjected to silica gel CC eluting with a CH<sub>2</sub>Cl<sub>2</sub>-EtOAc gradient system (95:5, 80:20, and 70:30, v/v) to yield five fractions, Fr.3-2-1–Fr.3-2-5. Fr. 3-2-2 (15.3 g) was separated on RP-C18 CC and eluted with MeOH-H<sub>2</sub>O (40:60–80:20, v/v) to afford four fractions, Fr.3-2-2-1–Fr.3-2-2-4. Fr.3-2-2-2 (2.5 g) was chromatographed on Sephadex LH-20 CC washing with MeOH and further separated by the semi-preparative HPLC (MeOH-H<sub>2</sub>O, 60:40, v/v, λ = 254/210 nm, 3.0 mL/min) to afford compounds **11** (t<sub>R</sub> = 15 min, 15 mg), **16** (t<sub>R</sub> = 17 min, 17 mg), **13** (t<sub>R</sub> = 18 min, 5 mg), and **12** (t<sub>R</sub> = 21 min, 7 mg). Fr.3-2-2-3 (1.7 g) was subjected to silica gel CC eluting with CH<sub>2</sub>Cl<sub>2</sub>-MeOH (98:2 and 95:5, v/v) and then isolated by semi-preparative HPLC (MeCN-H<sub>2</sub>O, 40:60, v/v, λ = 254/202 nm, 3.0 mL/min) to provide compounds **8** (t<sub>R</sub> = 16 min, 25 mg), **10** (t<sub>R</sub> = 18 min, 7

mg), **9** (t<sub>R</sub> = 19 min, 49 mg), and **7** (t<sub>R</sub> = 22 min, 8 mg). Fr. 3-2-3 (9.6 g) was isolated by RP-C8 CC eluted with MeOH-H<sub>2</sub>O (30:70–70:30, v/v) to afford five fractions, Fr.3-2-3-1–Fr.3-2-3-5. Fr.3-2-3-2 (1.1 g) was repeatedly separated on Sephadex LH-20 CC (MeOH) and semi-preparative HPLC (MeCN-H<sub>2</sub>O, 30:70 → 90:10, v/v, λ = 254/210 nm, 3.0 mL/min) to obtain compounds **5** (t<sub>R</sub> = 19 min, 21 mg), **6** (t<sub>R</sub> = 21 min, 28 mg), **14** (t<sub>R</sub> = 22 min, 5 mg), and **15** (t<sub>R</sub> = 25 min, 26 mg). Fr. 3-3-3-3 (3.3 g) was fractionated on a Rp-C18 CC (MeOH-H<sub>2</sub>O, 30:70, 50:50, 70:30, and 90:10, v/v), silica gel CC (petroleum ether-EtOAc, 10:90–70:30, v/v), semi-preparative HPLC with YMC-Pack ODS-A column (MeCN-H<sub>2</sub>O, 50:50, v/v, λ = 254/210 nm, 3.0 mL/min) to give out compounds **1** (t<sub>R</sub> = 17 min, 41 mg), **2** (t<sub>R</sub> = 18 min, 38 mg), **4** (t<sub>R</sub> = 20 min, 7 mg), and **3** (t<sub>R</sub> = 22 min, 11 mg).

**Jolkiniol A (1)**. White solids, C<sub>20</sub>H<sub>30</sub>O<sub>3</sub>, (+)-HR-ESI-MS [M + H]<sup>+</sup> m/z 319.2274 (calcd. 319.2268, +1.9 ppm); [α]<sub>D</sub><sup>23.7</sup> – 13.86 (c 0.07, MeOH); UV (MeOH) λ<sub>max</sub> (log ε) 203 (4.15), 280 (3.84) nm; IR (KBr) ν<sub>max</sub> 3372, 2926, 1615, 1458, 1386, 1277, 1057, 1022, 988, 902, 871, 615 cm<sup>-1</sup>; ECD (c 0.35, MeOH) λ<sub>max</sub> (Δε) 207 (+3.10), 212 (+2.96), 219 (+3.14), 242 (+3.73), 283 (–1.37), 306 (–0.76), 330 (–1.28) nm; <sup>1</sup>H and <sup>13</sup>C NMR data: see Table 1.

**Jolkiniol B (2)**. White solids, C<sub>20</sub>H<sub>30</sub>O<sub>3</sub>, (–)-HR-ESI-MS [M + Cl]<sup>–</sup> m/z 353.1884 (calcd. 353.1889, –1.3 ppm); [α]<sub>D</sub><sup>24.5</sup> + 11.08 (c 0.10, MeOH); UV (MeOH) λ<sub>max</sub> (log ε) 203 (3.75), 284 (3.43) nm; IR (KBr) ν<sub>max</sub> 3419, 2924, 1639, 1454, 1379, 1278, 1152, 1094, 1055, 884, 721 cm<sup>-1</sup>; ECD (c 0.50, MeOH) λ<sub>max</sub> (Δε) 228 (+0.26), 247 (+1.27), 266 (+0.77), 287 (+1.14), 334 (–1.66) nm; <sup>1</sup>H and <sup>13</sup>C NMR data: see Table 1.

**Jolkiniol C (3)**. White solids, C<sub>22</sub>H<sub>32</sub>O<sub>4</sub>, (+)-HR-ESI-MS [M + H]<sup>+</sup> m/z 361.2389 (calcd. 361.2373, +4.0 ppm); [α]<sub>D</sub><sup>25.9</sup> – 46.80 (c 0.10, MeOH); UV (MeOH) λ<sub>max</sub> (log ε) 228 (3.96) nm; IR (KBr) ν<sub>max</sub> 3444, 2936, 1739, 1667, 1448, 1386, 1237, 1040, 918, 828, 585 cm<sup>-1</sup>; ECD (c 0.33, MeOH), λ<sub>max</sub> (Δε) 207 (+5.08), 236 (–9.30), 342 (+2.08) nm; <sup>1</sup>H and <sup>13</sup>C NMR data: see Table 1.

**Jolkiniol D (4)**. White solids, C<sub>22</sub>H<sub>34</sub>O<sub>5</sub>, (–)-HR-ESI-MS [M +

**Table 1**

<sup>1</sup>H NMR (600 MHz) and <sup>13</sup>C NMR (150 MHz) spectroscopic data of **1–4** in CDCl<sub>3</sub> (δ in ppm, J in Hz).

Pos.	<b>1</b>		<b>2</b>		<b>3</b>		<b>4</b>	
	δ <sub>C</sub> , type	δ <sub>H</sub> (J)	δ <sub>C</sub> , type	δ <sub>H</sub> (J)	δ <sub>C</sub> , type	δ <sub>H</sub> (J)	δ <sub>C</sub> , type	δ <sub>H</sub> (J)
1	33.6, CH	1.15 (1H, overlapped)	38.0, CH	0.53 (1H, br.d, 13.6)	158.5, CH	6.92 (1H, d, 10.1)	39.4, CH <sub>2</sub>	α: 2.63–2.56 (1H, m) β: 1.66–1.61 (1H, m)
2	27.0, CH	1.48 (1H, t, 8.6)	32.2, CH	1.13 (1H, overlapped)	125.1, CH	5.81 (1H, d, 10.1)	34.2, CH <sub>2</sub>	α: 2.63–2.56 (1H, m) β: 2.41–2.35 (1H, m)
3	143.8, CH	6.26 (1H, d, 9.5)	148.6, CH	5.80 (1H, d, 10.3)	205.2, C	–	218.0, C	–
4	137.8, C	–	132.1, C	–	44.6, C	–	47.7, C	–
5	195.6, C	–	199.4, C	–	53.6, CH	1.63 (1H, m)	56.6, CH	1.31(1H, d, 10.7)
6	128.5, CH	6.42 (1H, d, 16.5)	129.6, CH	6.36 (1H, d, 16.0)	19.0, CH <sub>2</sub>	1.46–1.55 (2H, m)	19.8, CH <sub>2</sub>	1.56–1.49 (2H, m)
7	147.1, CH	6.63 (1H, d, 16.5)	154.3, CH	6.97 (1H, d, 16.0)	38.6, CH <sub>2</sub>	α: 1.46–1.48 (1H, m) β: 1.25–1.29 (1H, m)	38.4, CH <sub>2</sub>	α: 1.42–1.38 (1H, m) β: 1.16–1.10 (1H, m)
8	75.4, C	–	76.1, C	–	33.4, C	–	34.2, C	–
9	78.7, CH	3.70 (1H, br.s)	78.3, CH	3.82 (1H, br.s)	45.7, CH	1.59–1.61 (1H, m)	55.0, CH	1.45 (1H, d, 10.6)
10	31.7, CH <sub>2</sub>	2.38–2.42 (2H, m)	31.7, CH <sub>2</sub>	2.47–2.59 (2H, m)	40.1, C	–	38.2, C	–
11	119.8, CH	5.22 (1H, t, 6.8)	120.7, CH	5.43 (1H, br.s)	22.9, CH <sub>2</sub>	α: 1.37–1.40 (1H, m) β: 2.22–2.26 (1H, m)	66.9, CH	4.77 (1H, d, 10.3)
12	138.3, C	–	135.2, C	–	32.6, CH	1.84 (1H, t, 2.5)	42.2, CH	1.69 (1H, d, 2.3)
13	39.3, CH <sub>2</sub>	α: 2.24–2.30 (1H, m) β: 1.83 (1H, t, 11.4)	39.0, CH <sub>2</sub>	α: 2.28–2.32 (1H, m) β: 2.07–2.14 (1H, m)	23.1, CH <sub>2</sub>	α: 1.57–1.61 (1H, m) β: 1.50–1.54 (1H, m)	15.6, CH <sub>2</sub>	α: 2.06–2.00 (1H, m) β: 1.42–1.38 (1H, m)
14	25.5, CH <sub>2</sub>	α: 0.83–0.89 (1H, m) β: 2.12–2.17 (1H, m)	24.4, CH <sub>2</sub>	α: 1.25 (1H, br.s) β: 2.07–2.14 (1H, m)	27.5, CH <sub>2</sub>	α: 1.87–1.91 (1H, m) β: 0.84–0.90 (1H, m)	26.3, CH <sub>2</sub>	α: 1.98–1.94 (1H, m) β: 0.85–0.79 (1H, m)
15	26.0, C	–	27.1, C	–	52.0, CH <sub>2</sub>	1.25 (2H, s)	51.9, CH <sub>2</sub>	α: 1.23–1.21 (1H, m) β: 1.16–1.10 (1H, m)
16	29.0, CH <sub>3</sub>	1.18 (3H, s)	21.8, CH <sub>3</sub>	1.15 (3H, s)	72.7, C	–	72.3, C	–
17	16.1, CH <sub>3</sub>	1.01 (3H, s)	23.5, CH <sub>3</sub>	1.08 (3H, s)	70.1, CH <sub>2</sub>	4.11(1H, d, 11.4) 3.97 (1H, d, 11.4)	70.3, CH <sub>2</sub>	4.10 (1H, d, 11.5) 3.98 (1H, d, 11.5)
18	12.3, CH <sub>3</sub>	1.90 (3H, s)	12.8, CH <sub>3</sub>	1.88 (3H, s)	27.5, CH <sub>3</sub>	1.14 (3H, s)	26.7, CH <sub>3</sub>	1.06 (3H, s)
19	24.8, CH <sub>3</sub>	1.33 (3H, s)	24.7, CH <sub>3</sub>	1.28 (3H, s)	21.6, CH <sub>3</sub>	1.08 (3H, s)	21.5, CH <sub>3</sub>	1.04 (3H, s)
20	15.6, CH <sub>3</sub>	1.61 (3H, s)	14.1, CH <sub>3</sub>	0.62 (3H, s)	17.5, CH <sub>3</sub>	1.23 (3H, s)	16.6, CH <sub>3</sub>	1.37 (3H, s)
–COCH <sub>3</sub>					171.1, C	–	171.2, C	–
–COCH <sub>3</sub>					20.9, CH <sub>3</sub>	2.11 (3H, s)	20.9, CH <sub>3</sub>	2.10 (3H, s)

HCOO<sup>-</sup>  $m/z$  423.2378 (calcd. 423.2388,  $-2.2$  ppm); [ $\alpha$ ]<sub>D</sub><sup>25.2</sup>  $-6.48$  (c 0.05, MeOH); UV (MeOH)  $\lambda_{\max}$  (log  $\epsilon$ ) 202 (2.97), 265 (2.04) nm; IR (KBr)  $\nu_{\max}$  3432, 2931, 1702, 1449, 1384, 1250, 1051 cm<sup>-1</sup>; ECD (c 0.50, MeOH)  $\lambda_{\max}$  ( $\Delta\epsilon$ ) 211 (+0.31) nm; <sup>1</sup>H and <sup>13</sup>C NMR data: see Table 1.

**Jolkiniol E (5).** White solids, C<sub>20</sub>H<sub>28</sub>O<sub>3</sub>, (+)-HR-ESI-MS [M + H]<sup>+</sup>  $m/z$  317.2112 (calcd. 317.2111, +0.7 ppm); [ $\alpha$ ]<sub>D</sub><sup>24.8</sup> + 10.72 (c 0.05, MeOH); UV (MeOH)  $\lambda_{\max}$  (log  $\epsilon$ ) 202 (3.60), 224 (3.52) nm; IR (KBr)  $\nu_{\max}$  3431, 2928, 1671, 1382, 1273, 1004, 830, 580 cm<sup>-1</sup>; ECD (c 0.50, MeOH)  $\lambda_{\max}$  ( $\Delta\epsilon$ ) 210 (+3.61), 242 ( $-0.28$ ) nm, 355 (+0.34); <sup>1</sup>H and <sup>13</sup>C NMR data: see Table 2.

**Jolkiniol F (6).** White solids, C<sub>20</sub>H<sub>28</sub>O<sub>3</sub>, HR-ESI-MS [M + H]<sup>+</sup>  $m/z$  317.2115 (calcd. 317.2111, +0.9 ppm); [ $\alpha$ ]<sub>D</sub><sup>24.9</sup> + 20.96 (c 0.06, MeOH); UV (MeOH)  $\lambda_{\max}$  (log  $\epsilon$ ) 203 (3.92), 267 (3.80) nm; IR (KBr)  $\nu_{\max}$  3410, 2971, 1647, 1410, 1221, 1059, 915, 643 cm<sup>-1</sup>; ECD (c 0.30, MeOH)  $\lambda_{\max}$  ( $\Delta\epsilon$ ) 202 (+5.92), 224 (+0.60), 245 (+0.90), 285 ( $-0.12$ ), 332 (+0.54) nm; <sup>1</sup>H and <sup>13</sup>C NMR data: see Table 2.

**Jolkiniol G (7).** White solids, C<sub>22</sub>H<sub>30</sub>O<sub>4</sub>, (+)-HR-ESI-MS [M + H]<sup>+</sup>  $m/z$  359.2208 (calcd. 359.2217,  $-2.5$  ppm); [ $\alpha$ ]<sub>D</sub><sup>24.3</sup> + 5.17 (c 0.06, MeOH); UV (MeOH)  $\lambda_{\max}$  (log  $\epsilon$ ) 202 (3.05), 215 (2.88) nm; IR (KBr)  $\nu_{\max}$  3439, 2924, 1637, 1383, 1043, 668 cm<sup>-1</sup>; ECD (c 0.60, MeOH)  $\lambda_{\max}$  ( $\Delta\epsilon$ ) 199 (+1.56), 233 ( $-0.24$ ), 355 (+0.31) nm; <sup>1</sup>H and <sup>13</sup>C NMR data: see Table 2.

**Jolkiniol H (8).** White solids, C<sub>22</sub>H<sub>32</sub>O<sub>3</sub>, (+)-HR-ESI-MS [M + Na]<sup>+</sup>  $m/z$  367.2248 (calcd. 367.2244, +1.0 ppm), [ $\alpha$ ]<sub>D</sub><sup>25.2</sup>  $-32.00$  (c 0.10, MeOH); UV (MeOH)  $\lambda_{\max}$  (log  $\epsilon$ ) 205 (3.78), 224 (3.81) nm; IR (KBr)  $\nu_{\max}$  3436, 2971, 1716, 1668, 1455, 1385, 1262, 1064, 830, 581 cm<sup>-1</sup>; ECD (c 0.43, MeOH)  $\lambda_{\max}$  ( $\Delta\epsilon$ ) 204 (+0.37), 222 ( $-3.41$ ), 256 (+0.63), 348 (+0.41) nm; <sup>1</sup>H and <sup>13</sup>C NMR data: see Table 2.

**Jolkiniol I (9).** White solids, C<sub>22</sub>H<sub>32</sub>O<sub>3</sub>, (+)-HR-ESI-MS [M + H]<sup>+</sup>  $m/z$  345.2427 (calcd. 345.2424, +0.6 ppm), [ $\alpha$ ]<sub>D</sub><sup>24.4</sup>  $-25.73$  (c 0.09, MeOH);

UV (MeOH)  $\lambda_{\max}$  (log  $\epsilon$ ) 203 (3.46), 225 (3.53) nm; IR (KBr)  $\nu_{\max}$  3435, 2969, 1453, 1384, 1075, 831, 568 cm<sup>-1</sup>; ECD (c 0.69, MeOH)  $\lambda_{\max}$  ( $\Delta\epsilon$ ) 207 ( $-1.38$ ), 226 ( $-4.36$ ), 263 (+0.19), 344 (+0.56) nm; <sup>1</sup>H and <sup>13</sup>C NMR data: see Table 3.

**Jolkiniol J (10).** White solids, C<sub>22</sub>H<sub>32</sub>O<sub>3</sub>, (+)-HR-ESI-MS [M + H]<sup>+</sup>  $m/z$  345.2433 (calcd. 345.2424, +2.5 ppm); [ $\alpha$ ]<sub>D</sub><sup>25.3</sup>  $-10.00$  (c 0.10, MeOH); UV (MeOH)  $\lambda_{\max}$  (log  $\epsilon$ ) 201 (2.02) nm; IR (KBr)  $\nu_{\max}$  3437, 2923, 1637, 1383, 1047, 373 cm<sup>-1</sup>; ECD (c 1.00, MeOH)  $\lambda_{\max}$  ( $\Delta\epsilon$ ) 225 ( $-0.27$ ), 355 (+0.39); <sup>1</sup>H and <sup>13</sup>C NMR data: see Table 3.

**Jolkiniol K (11).** White solids, C<sub>20</sub>H<sub>30</sub>O<sub>3</sub>, (+)-HR-ESI-MS [M + H]<sup>+</sup>  $m/z$  319.2270 (calcd. 319.2268, +0.6 ppm); [ $\alpha$ ]<sub>D</sub><sup>24.0</sup> + 10.80 (c 0.10, MeOH); UV (MeOH)  $\lambda_{\max}$  (log  $\epsilon$ ) 203 (3.65), 238 (2.83) nm; IR (KBr)  $\nu_{\max}$  3434, 2970, 1716, 1636, 1390, 1111, 1058, 921, 587 cm<sup>-1</sup>; ECD (c 0.33, MeOH)  $\lambda_{\max}$  ( $\Delta\epsilon$ ) 226 (+0.15), 248 (+0.42) nm; <sup>1</sup>H and <sup>13</sup>C NMR data: see Table 3.

**Jolkiniol L (12).** White solids, C<sub>20</sub>H<sub>30</sub>O<sub>3</sub>, (+)-HR-ESI-MS [M + H]<sup>+</sup>  $m/z$  319.2270 (calcd. 319.2268, +0.6 ppm); [ $\alpha$ ]<sub>D</sub><sup>24.8</sup>  $-56.32$  (c 0.10, MeOH); UV (MeOH)  $\lambda_{\max}$  (log  $\epsilon$ ) 204 (3.96), 239 (3.27) nm; IR (KBr)  $\nu_{\max}$  3456, 2954, 1701, 1388, 1280, 1117, 1055, 926, 657 cm<sup>-1</sup>; ECD (c 0.33, MeOH)  $\lambda_{\max}$  ( $\Delta\epsilon$ ) 229 (+0.65), 289 ( $-0.56$ ) nm; <sup>1</sup>H and <sup>13</sup>C NMR data: see Table 3.

**Jolkiniol M (13).** White solids, C<sub>20</sub>H<sub>28</sub>O<sub>3</sub>, (+)-HR-ESI-MS [M + Na]<sup>+</sup>  $m/z$  339.1932 (calcd. 339.1931, +0.3 ppm); [ $\alpha$ ]<sub>D</sub><sup>24.1</sup> + 8.04 (c 0.05, MeOH); UV (MeOH)  $\lambda_{\max}$  (log  $\epsilon$ ) 200 (3.20), 240 (3.47) nm; IR (KBr)  $\nu_{\max}$  3432, 2968, 2927, 1714, 1634, 1386, 1064, 596 cm<sup>-1</sup>; ECD (c 0.50, MeOH)  $\lambda_{\max}$  ( $\Delta\epsilon$ ) 205 (+0.21), 235 (+0.79) nm; <sup>1</sup>H and <sup>13</sup>C NMR data: see Table 4.

**Jolkiniol N (14).** White solids, C<sub>20</sub>H<sub>26</sub>O<sub>4</sub>, (+)-HR-ESI-MS [M + H]<sup>+</sup>  $m/z$  331.1915 (calcd. 331.1904, +1.4 ppm); [ $\alpha$ ]<sub>D</sub><sup>25.2</sup> + 3.84 (c 0.05, MeOH); UV (MeOH)  $\lambda_{\max}$  (log  $\epsilon$ ) 202 (3.01), 215 (2.94), 238 (2.88) nm; IR (KBr)  $\nu_{\max}$  3433, 2927, 1718, 1668, 1383, 1113, 585 cm<sup>-1</sup>; ECD (c

Table 2

<sup>1</sup>H NMR (600 MHz) and <sup>13</sup>C NMR (150 MHz) spectroscopic data of 5–8 in CDCl<sub>3</sub> ( $\delta$  in ppm,  $J$  in Hz).

Pos.	5		6		7		8	
	$\delta_C$ , type	$\delta_H$ ( $J$ )	$\delta_C$ , type	$\delta_H$ ( $J$ )	$\delta_C$ , type	$\delta_H$ ( $J$ )	$\delta_C$ , type	$\delta_H$ ( $J$ )
1	154.0, CH	6.92 (1H, d, 10.2)	123.6, CH	6.21 (1H, s)	154.9, CH	6.95 (1H, d, 10.2)	154.8, CH	7.17 (1H, d, 10.3)
2	125.7, CH	5.93 (1H, d, 10.2)	143.6, C	–	126.9, CH	5.95 (1H, d, 10.2)	126.7, CH	5.91 (1H, d, 10.3)
3	204.2, C	–	200.5, C	–	204.5, C	–	204.2, C	–
4	43.9, C	–	43.4, C	–	44.0, C	–	44.1, C	–
5	47.8, CH	1.98 (1H, dd, 11.0/5.1)	48.0, CH	1.85 (1H, dd, 11.8/3.7)	43.9, CH	2.46 (1H, dd, 10.9/2.4)	46.2, CH	1.96 (1H, overlapped)
6	22.9, CH <sub>2</sub>	2.14 (2H, m)	22.7, CH <sub>2</sub>	$\alpha$ : 1.98–2.00 (1H, m) $\beta$ : 2.07–2.12 (1H, m)	29.2, CH <sub>2</sub>	$\alpha$ : 1.85–1.90 (1H, m) $\beta$ : 1.79 (1H, td, 14.2/2.3)	25.9, CH <sub>2</sub>	$\alpha$ : 1.65–1.71 (1H, m) $\beta$ : 2.17 (1H, dd, 11.8/7.6)
7	127.7, CH	5.88 (1H, br.s)	122.6, CH	5.51 (1H, d, 4.9)	72.2, CH	4.40 (1H, br.s)	78.9, CH	3.83 (1H, t, 7.0)
8	136.8, C	–	133.4, C	–	138.2, C	–	128.8, C	–
9	37.7, CH	2.71 (1H, d, 11.5)	47.6, CH	2.07–2.12 (1H, m)	39.9, CH	2.60 (1H, t, 6.3)	135.0, C	–
10	36.8, C	–	36.3, C	–	40.8, C	–	40.8, C	–
11	27.1, CH <sub>2</sub>	$\alpha$ : 1.78 (1H, td, 13.5/2.3) $\beta$ : 2.03–2.06 (1H, m)	27.3, CH <sub>2</sub>	$\alpha$ : 1.42–1.48 (1H, m) $\beta$ : 1.92–1.96 (1H, m)	23.5, CH <sub>2</sub>	$\alpha$ : 1.93–1.98 (1H, m) $\beta$ : 1.85–1.90 (1H, m)	32.0, CH <sub>2</sub>	$\alpha$ : 2.45 (1H, dd, 16.7/5.2) $\beta$ : 2.01 (1H, overlapped)
12	74.5, CH	3.98 (1H, br.s)	73.8, CH	3.53 (1H, dd, 11.5/4.2)	75.2, CH	4.88 (1H, dd, 8.7/3.4)	73.9, CH	3.62 (1H, dd, 9.6/5.4)
13	43.6, C	–	42.7, C	–	41.3, C	–	40.2, C	–
14	81.7, CH	3.96 (1H, s)	45.5, CH <sub>2</sub>	2.02–2.04 (2H, m)	132.4, CH	5.60 (1H, s)	38.8, CH <sub>2</sub>	$\alpha$ : 2.32 (1H, d, 18.5) $\beta$ : 1.97 (1H, overlapped)
15	142.7, CH	6.30 (1H, dd, 17.8, 11.0)	146.1, CH	5.75 (1H, dd, 17.5, 10.8)	141.4, CH	5.82 (1H, dd, 17.4/10.6)	140.0, CH	5.84 (1H, dd, 17.6/10.9)
16	114.4, CH <sub>2</sub>	5.34 (1H, d, 17.8) 5.29 (1H, d, 11.0)	114.5, CH <sub>2</sub>	5.16 (2H, t, 14.9)	115.0, CH <sub>2</sub>	5.14 (1H, d, 10.6) 5.00 (1H, d, 17.4)	115.1, CH <sub>2</sub>	5.15 (1H, d, 10.9) 5.05 (1H, d, 17.6)
17	22.1, CH <sub>3</sub>	0.88 (3H, s)	13.7, CH <sub>3</sub>	0.91 (3H, s)	25.6, CH <sub>3</sub>	1.15 (3H, s)	23.7, CH <sub>3</sub>	1.15 (3H, s)
18	25.0, CH <sub>3</sub>	1.16 (3H, s)	25.3, CH <sub>3</sub>	1.20 (3H, s)	26.6, CH <sub>3</sub>	1.18 (3H, s)	26.6, CH <sub>3</sub>	1.17 (3H, s)
19	22.8, CH <sub>3</sub>	1.13 (3H, s)	22.4, CH <sub>3</sub>	1.16 (3H, s)	21.9, CH <sub>3</sub>	1.09 (3H, s)	21.4, CH <sub>3</sub>	1.11 (3H, s)
20	14.6, CH <sub>3</sub>	1.08 (3H, s)	15.8, CH <sub>3</sub>	1.11 (3H, s)	16.0, CH <sub>3</sub>	1.08 (3H, s)	24.1, CH <sub>3</sub>	1.27 (3H, s)
	–COCH <sub>3</sub>				170.8, C	–		
	–COCH <sub>3</sub>				21.2, CH <sub>3</sub>	2.03 (3H, s)		
	–OCH <sub>2</sub> CH <sub>3</sub>						64.3, CH <sub>2</sub>	3.71 (1H, dq, 14.0/7.0) 3.46 (1H, dq, 14.1/7.0)
	–OCH <sub>2</sub> CH <sub>3</sub>						15.7, CH <sub>3</sub>	1.24 (3H, t, 7.0)

**Table 3**<sup>1</sup>H NMR (600 MHz) and <sup>13</sup>C NMR (150 MHz) spectroscopic data of **9–12** in CDCl<sub>3</sub> ( $\delta$  in ppm, *J* in Hz).

Pos.	<b>9</b>		<b>10</b>		<b>11</b>		<b>12</b>	
	$\delta_C$ , type	$\delta_H$ ( <i>J</i> )	$\delta_C$ , type	$\delta_H$ ( <i>J</i> )	$\delta_C$ , type	$\delta_H$ ( <i>J</i> )	$\delta_C$ , type	$\delta_H$ ( <i>J</i> )
1	154.6, CH	7.15 (1H, d, 10.3)	154.5, CH	7.19 (1H, d, 10.3)	51.3, CH <sub>2</sub>	$\alpha$ : 2.57 (1H, d, 12.9) $\beta$ : 2.26 (1H, d 12.9)	50.9, CH <sub>2</sub>	$\alpha$ : 2.43 (1H, d, 12.7) $\beta$ : 2.29 (1H, d 12.6)
2	127.0, CH	5.91(1H, d, 10.3)	127.0, CH	5.93 (1H, d, 10.2)	210.5, C	–	210.5, C	–
3	204.7, C	–	204.6, C	–	82.3, CH	3.93(1H, s)	82.5, CH	3.96 (1H, d)
4	43.9, C	–	43.9, C	–	45.0, C	–	45.6, C	–
5	42.5, CH	2.30 (1H, dd, 13.1/1.4)	42.6, CH	2.29 (1H, br.d, 15.3)	50.9, CH	2.16 (1H, d, 12.1)	52.9, CH	1.68 (1H, d, 12.4)
6	23.9, CH <sub>2</sub>	$\alpha$ : 1.65 (1H, td, 13.7/4.2) $\beta$ : 1.93 (1H, d, 14.1)	24.0, CH <sub>2</sub>	$\beta$ : 1.94 (1H, d, 14.3) $\alpha$ : 1.67 (1H, td, 13.7/4.2)	23.3, CH <sub>2</sub>	1.98–2.06 (2H, m)	21.9, CH <sub>2</sub>	$\alpha$ : 1.75 (1H, dd, 13.1/2.7) $\beta$ : 1.44–1.48 (1H, m) $\alpha$ : 2.43 (1H, d, 12.7) $\beta$ : 2.13 (1H, td, 12.6/4.9)
7	74.8, CH	3.50 (1H, d, 2.4)	74.6, CH	3.50 (1H, br.s)	122.3, CH	5.44 (1H, s)	34.2, CH <sub>2</sub>	–
8	128.0, C	–	128.0, C	–	133.2, C	–	136.3, C	–
9	134.7, C	–	134.7, C	–	48.8, CH	1.77 (1H, dd, 11.4/4.1)	51.9, CH	2.24 (1H, t, 9.4)
10	40.9, C	–	41.1, C	–	42.4, C	–	44.4, C	–
11	31.5, CH <sub>2</sub>	$\alpha$ : 2.43 (1H, dd, 16.6/5.0) $\beta$ : 2.03 (1H, dd, 15.9/10.4)	29.2, CH <sub>2</sub>	$\alpha$ : 2.10–2.17 (1H, m) $\beta$ : 2.49 (1H, dd, 17.0/5.5)	27.4, CH <sub>2</sub>	$\alpha$ : 1.35 (1H, t, 12.2) $\beta$ : 1.65 (1H, dd, 11.4/5.2)	28.4, CH <sub>2</sub>	$\alpha$ : 1.39–1.40 (1H, m) $\beta$ : 1.60 (1H, overlapped)
12	74.4, CH	3.58 (1H, td, 9.3/7.1)	72.0, CH	3.60–3.66 (1H, m)	73.7, CH	3.50 (1H, dd, 11.5/3.7)	75.5, CH	3.46 (1H, d, 11.8)
13	40.3, C	–	40.9, C	–	42.0, C	–	43.9, C	–
14	39.6, CH <sub>2</sub>	$\alpha$ : 1.88 (1H, d, 17.5) $\beta$ : 2.53 (1H, d, 17.3)	40.3, CH <sub>2</sub>	$\alpha$ : 2.29 (1H, d, 17.5) $\beta$ : 1.98 (1H, d, 17.7)	44.9, CH <sub>2</sub>	1.98–2.06 (2H, m)	128.6, CH	5.12 (1H, s)
15	139.8, CH	5.87 (1H, dd, 17.6/10.9)	145.7, CH	5.78 (1H, dd, 17.3/10.8)	146.6, CH	5.73 (1H, dd, 17.5/10.8)	141.4, CH	5.87 (1H, dd, 17.5/10.6)
16	115.6, CH <sub>2</sub>	5.17 (2H, t, 13.5)	115.2, CH <sub>2</sub>	5.21 (2H, t, 13.4)	114.4, CH <sub>2</sub>	5.08–5.17 (2H, m)	117.0, CH <sub>2</sub>	5.21 (1H, d, 10.6) 5.07 (1H, d, 17.5)
17	23.8, CH <sub>3</sub>	1.14 (3H, s)	14.4, CH <sub>3</sub>	0.98 (3H, s)	13.6, CH <sub>3</sub>	0.84 (3H, s)	24.9, CH <sub>3</sub>	1.15 (3H, s)
18	26.8, CH <sub>3</sub>	1.17 (3H, s)	26.8, CH <sub>3</sub>	1.17 (3H, s)	28.5, CH <sub>3</sub>	1.13 (3H, s)	29.7, CH <sub>3</sub>	1.25 (3H, s)
19	21.5, CH <sub>3</sub>	1.11 (3H, s)	21.5, CH <sub>3</sub>	1.12 (3H, s)	16.3, CH <sub>3</sub>	0.74 (3H, s)	16.6, CH <sub>3</sub>	0.70 (3H, s)
20	23.0, CH <sub>3</sub>	1.16 (3H, s)	23.0, CH <sub>3</sub>	1.17 (3H, s)	15.4, CH <sub>3</sub>	0.88 (3H, s)	15.0, CH <sub>3</sub>	0.78 (3H, s)
–OCH <sub>2</sub> CH <sub>3</sub>	64.8, CH <sub>2</sub>	3.65 (1H, dq, 14.1/7.0) 3.41 (1H, dq, 14.1/7.0)	64.8, CH <sub>2</sub>	3.60–3.66 (1H, m) 3.34–3.43 (1H, m)				
–OCH <sub>2</sub> CH <sub>3</sub>	15.0, CH <sub>3</sub>	1.20 (3H, t, 7.0)	15.6, CH <sub>3</sub>	1.19 (3H, t, 7.0)				

0.50, MeOH)  $\lambda_{\max}$  ( $\Delta\epsilon$ ) 221 (+0.36), 249 (+0.10) nm; <sup>1</sup>H and <sup>13</sup>C NMR data: see Table 4.

**Jolkiniol O (15)**, white solids, C<sub>20</sub>H<sub>26</sub>O<sub>3</sub>, (+)-HR-ESI-MS [M + H]<sup>+</sup> *m/z* 315.1960 (calcd. 315.1955, +1.3 ppm); [ $\alpha$ ]<sub>D</sub><sup>25.4</sup> + 98.40 (c 0.15, MeOH); UV (MeOH)  $\lambda_{\max}$  (log  $\epsilon$ ) 202 (3.85), 229 (3.79), 290 (3.79) nm; IR (KBr)  $\nu_{\max}$  3437, 2972, 1719, 1669, 1454, 1394, 1264, 1194, 1113, 1070, 928 cm<sup>-1</sup>; ECD (c 0.45, MeOH)  $\lambda_{\max}$  ( $\Delta\epsilon$ ) 212 (–1.86), 288 (+5.47), 336 (–0.57) nm; <sup>1</sup>H and <sup>13</sup>C NMR data: see Table 4.

**Jolkiniol P (16)**, white solids, C<sub>20</sub>H<sub>32</sub>O<sub>2</sub>, (+)-HR-ESI-MS [M + H]<sup>+</sup> *m/z* 305.2462. (calcd. 305.2475, –4.3 ppm); [ $\alpha$ ]<sub>D</sub><sup>24.1</sup> – 21.6 (c 0.05, MeOH); UV (MeOH)  $\lambda_{\max}$  (log  $\epsilon$ ) 204 (3.58) nm; IR (KBr)  $\nu_{\max}$  3429, 2930, 1719, 1633, 1457, 1385, 1035, 919, 556 cm<sup>-1</sup>; ECD (c 0.33, MeOH)  $\lambda_{\max}$  ( $\Delta\epsilon$ ) 248 (+0.23) nm; <sup>1</sup>H and <sup>13</sup>C NMR data: see Table 4.

#### 2.4. Cytotoxicity assay

The cytotoxicity of the compounds was detected by CKK-8 method. Pancreatic cancer cells were cultured in a 5 % carbon dioxide incubator containing at 37 °C. The culture mediums were composed of 89 % DMEM, 10 % fetal bovine serum, and 1 % penicillin–streptomycin solution. The cells were digested with 2 mL trypsin for 2 min when the density of cells on the petri dish was greater than 85 %. And then the cells were added with 4 mL mediums and transferred to a 15 mL centrifuge tube via trypsin for centrifugation. The cells were inoculated into a 96-well plate with 100  $\mu$ L per well after centrifugation and inoculated continuously for 24 h. Then the cells were treated with the compounds and paclitaxel as positive control. The CCK-8 reagents were diluted ten-fold with DMEM medium 24 h later and the cells were cultivated for 2 h. Finally, the absorbances were measured by a microplate reader at 450 nm. Inhibition ratios were calculated as  $[A_{\text{control}} -$

$A_{\text{sample}}]/A_{\text{control}} \times 100$  %. The IC<sub>50</sub> values were calculated according to Prism.8 software.

#### 2.5. Flow cytometric analysis

Fluorescein FITC-labelled Annexin-V is applied to label the early apoptotic cells due to its high combining capacity with the phosphatidylserine in early apoptotic cells. Propidium Iodide (PI), a nucleic acid dye, is not permeable to the normal cell membranes. But it can through the membranes of apoptotic cells at middle and late-stage (Wei et al., 2023). Thus, Annexin-V and PI are utilized to detect apoptotic cells to determine the cell cycles. Firstly, the tumor cells were inoculated in 6-well plates at an inoculum density of  $2 \times 10^6$  cells/well. 24 h later, compounds **1** (13  $\mu$ M, 26  $\mu$ M), **9** (11  $\mu$ M, 22  $\mu$ M), and positive drug (paclitaxel 45  $\mu$ M) were added. After 3 h, the cells were transferred to a 5 mL centrifuge tube via trypsin for centrifugation. Then FITC (5  $\mu$ L) and PI (5  $\mu$ L) were added sequentially into the cells for the incubation at room temperature of 15 min. Then 400  $\mu$ L PBS were added to each culture tube, and the cells were subjected to the flow cytometer. The data were analyzed by FlowJo\_v10.8.1 software.

#### 2.6. Western blot assay

The Western blot assay was prepared according to our previous report (Chen et al., 2022). The cell culture procedures were similar with cytotoxicity assay. According to the IC<sub>50</sub> values, the concentrations of the samples were set as: 2.5  $\mu$ M, 5  $\mu$ M, and 10  $\mu$ M for compound **1**, 3  $\mu$ M, 6  $\mu$ M, and 12  $\mu$ M for compound **9** and 20  $\mu$ M for positive control. The mediums were removed 3 h later. Then the RIPA lysis buffer (protease inhibitor: EDTA = 98:1:1) was added to lyse the cells for 1 h. After the

**Table 4**<sup>1</sup>H NMR (600 MHz) and <sup>13</sup>C NMR (150 MHz) spectroscopic data of **13–16** in CDCl<sub>3</sub> ( $\delta$  in ppm, *J* in Hz).

Pos.	<b>13</b>		<b>14</b>		<b>15</b>		<b>16</b>	
	$\delta_C$ , type	$\delta_H$ ( <i>J</i> )	$\delta_C$ , type	$\delta_H$ ( <i>J</i> )	$\delta_C$ , type	$\delta_H$ ( <i>J</i> )	$\delta_C$ , type	$\delta_H$ ( <i>J</i> )
1	49.7, CH <sub>2</sub>	$\alpha$ : 2.52 (1H, d, 12.6) $\beta$ : 2.34 (1H, d, 12.4)	50.2, CH <sub>2</sub>	$\alpha$ : 2.70 (1H, d, 12.3) $\beta$ : 2.54 (1H, s, 12.4)	48.9, CH <sub>2</sub>	$\alpha$ : 2.69 (1H, d, 12.6) $\beta$ : 2.61 (1H, s, 13.2)	36.8, CH <sub>2</sub>	$\alpha$ : 1.62 (1H, m) $\beta$ : 1.14–1.18 (m)
2	210.2, C	–	208.8, C	–	209.5, C	–	26.1, CH <sub>2</sub>	1.62 (2H, m)
3	82.6, CH	3.96 (1H, d, 2.4)	81.9, CH	3.91 (1H, s)	82.0, CH	3.96 (1H, d, 1.1)	79.0, CH	3.26 (d, <i>J</i> = 9.1 Hz, 1H)
4	44.5, C	–	44.8, C	–	44.9, C	–	39.0, C	–
5	53.4, CH	2.65 (1H, s)	47.5, CH	1.89 (1H, dd, 13.0/5.4)	46.3, CH	1.99 (1H, dd, 11.4/4.6)	54.2, CH	1.08 (0)
6	126.1, CH	5.68 (1H, d, 9.3)	21.7, CH <sub>2</sub>	$\alpha$ : 2.14 (1H, d, 13.1) $\beta$ : 2.29 (1H, dt, 15.4/5.7)	22.5, CH <sub>2</sub>	$\alpha$ : 2.32–2.24 (1H, m) $\beta$ : 2.47 (1H, dt, 19.1/4.4)	22.2, CH <sub>2</sub>	$\alpha$ : 1.62 (m) $\beta$ : 1.40–1.44 (m)
7	130.7, CH	6.12 (1H, d, 7.4)	60.1, CH	3.47 (1H, d, 6.0)	130.8, CH	6.11 (1H, d, 3.1)	35.4, CH <sub>2</sub>	$\alpha$ : 2.09 (td, <i>J</i> = 13.6/4.5 Hz, 1H) $\beta$ : 2.36 (dd, <i>J</i> = 14.3/2.5 Hz)
8	133.5, C	–	54.9, C	–	129.4, C	–	138.1, C	–
9	49.8, CH	2.55 (1H, overlapped)	163.0, C	–	163.1, C	–	46.3, CH	1.84 (t, <i>J</i> = 8.3 Hz, 1H)
10	42.8, C	–	44.0, C	–	43.0, C	–	38.2, C	–
11	26.3, CH <sub>2</sub>	$\alpha$ : 1.53 (1H, overlapped) $\beta$ : 1.67–1.70 (1H, m)	125.0, CH	5.93 (1H, s)	117.6, CH	5.59 (1H, s)	27.5, CH <sub>2</sub>	1.62 (2H, m)
12	73.3, CH	3.72 (1H, d, 11.1)	202.1, C	–	201.6, C	–	72.8, CH	3.64 (s, 1H)
13	44.1, C	–	47.7, C	–	48.7, C	–	43.8, C	–
14	133.3, CH	5.34 (1H, s)	41.3, CH <sub>2</sub>	$\alpha$ : 1.63 (1H, s) $\beta$ : 2.56 (1H, d, 3.4)	43.6, CH <sub>2</sub>	$\alpha$ : 2.61 (1H, d, 13.2) $\beta$ : 2.55 (1H, 14.3)	124.6, CH	5.07 (s, 1H)
15	145.0, CH	5.83 (1H, dd, 17.4/10.7)	140.8, CH	6.14 (1H, dd, 17.6/10.8)	140.0, CH	5.82 (1H, dd, 17.5/10.7)	146.2, CH	5.74 (dd, <i>J</i> = 17.0/10.7 Hz, 1H)
16	114.3, CH <sub>2</sub>	5.15 (2H, dd, 13.9/11.3)	114.0, CH <sub>2</sub>	5.19 (1H, d, 10.8) 5.07 (1H, d, 17.6)	114.9, CH <sub>2</sub>	5.07 (1H, d, 10.7) 5.05 (1H, d, 17.5)	114.1, CH <sub>2</sub>	5.02 (d, <i>J</i> = 6.4 Hz, 1H) 5.00 (s, 1H)
17	18.6, CH <sub>3</sub>	1.09 (3H, s)	23.7, CH <sub>3</sub>	1.37 (3H, s)	22.5, CH <sub>3</sub>	1.21 (3H, s)	23.5, CH <sub>3</sub>	1.08 (s, 3H)
18	28.8, CH <sub>3</sub>	1.26 (3H, s)	28.5, CH <sub>3</sub>	1.21 (3H, s)	27.9, CH <sub>3</sub>	1.19 (3H, s)	28.5, CH <sub>3</sub>	1.02 (s, 3H)
19	16.9, CH <sub>3</sub>	0.73 (3H, s)	15.9, CH <sub>3</sub>	0.75 (3H, s)	16.2, CH <sub>3</sub>	0.80 (3H, s)	15.7, CH <sub>3</sub>	0.82 (s, 3H)
20	14.1, CH <sub>3</sub>	0.72 (3H, s)	23.0, CH <sub>3</sub>	1.17 (3H, s)	21.3, CH <sub>3</sub>	1.04 (3H, s)	14.7, CH <sub>3</sub>	0.75 (s, 3H)

centrifugation at 13,200 rpm  $\times$  30 min, the supernatants were collected and 1/3 vol of protein buffer ( $\beta$ -hydrophobic ethanol: 4  $\times$  SDS concentrated gel buffer solution = 1:9) were added. The supernatants were subjected to heat denaturation at 95 °C for 5 min and stored at –20 °C refrigerator. 30  $\mu$ g proteins were added in SDS-PAGE and electroblotted onto PVDF membrane. The membranes were blocked with 5 % skim milk in TBS-T, and probed with desired antibodies. Super Signal West Dura Extended Duration Substrate (Pierce, Rockford, IL, USA) was used to detect antibody-antigen complexes. The data were collated and analyzed by ChemiScope Analysis and Prism.8 software.

## 2.7. Molecular docking and druggability prediction

The molecular docking assay was prepared according to our previous report (Yang et al., 2023). The 3D structure of Bcl-2 protein was downloaded from Protein Data Bank (PDB, <https://www.rcsb.org>). Molecular docking was conducted using Discovery Studio 4.0 software. LibDockScores of compounds with target proteins were used to evaluate their affinity and the docking results were drawn using PyMol software. Discovery Studio 2016 Client software was used to predict the pharmacokinetics of the compounds.

## 2.8. Statistical analysis

All the data were statistically analyzed by using GraphPad prism 8.0 statistical software and expressed as mean  $\pm$  standard deviations (SDs). Multiple comparisons between groups were performed using one-way ANOVA, and pairwise comparisons were conducted by independent *t*-test. In all cases, differences with *P* < 0.05 were considered statistically significant.

## 3. Results and discussions

### 3.1. Structure elucidation

Compound **1** was obtained as white solids with the molecular formula as C<sub>20</sub>H<sub>30</sub>O<sub>3</sub> which was determined by the (+)-HR-ESI-MS at *m/z* 319.2274 ([M + H]<sup>+</sup> calcd. 319.2268) indicating six unsaturation degrees. The <sup>1</sup>H NMR spectrum of **1** exhibited four olefinic protons at  $\delta_H$  5.22 (1H, t, *J* = 6.8 Hz), 6.26 (1H, d, *J* = 9.5 Hz), 6.42 (1H, d, *J* = 16.5 Hz), and 6.63 (1H, d, *J* = 16.5 Hz) and five methyl signals at  $\delta_H$  1.01 (3H, s), 1.18 (3H, s), 1.33 (3H, s), 1.61 (3H, s), and 1.90 (3H, s) (Table 1). The <sup>13</sup>C NMR spectrum presented 20 carbons including five methyls, three methylenes, seven methines, and five quaternary carbons from which a carbonyl unit at  $\delta_C$  195.6 and three double bonds at  $\delta_C$  147.1 (CH), 143.8 (CH), 138.3 (C), 137.8 (C), 128.5 (CH), and 119.8 (CH) were deduced. Thus, the remaining two unsaturation degrees required by the molecular formula of **1** were attributed to two rings. The presence of a quaternary carbon at  $\delta_C$  26.0 (C-15) and a *gem*-dimethyl functionality at  $\delta_C$  29.0 (C-16)/16.1 (C-17), together with the <sup>1</sup>H–<sup>1</sup>H-COSY correlations between two cyclopropyl protons of H-1 ( $\delta_H$  1.15, overlapped) and H-2 ( $\delta_H$  1.48, t, 8.6), indicated the presence of a substituted cyclopropyl ring (Fig. 2). Consequently, compound **1** was deduced to be a casbane diterpenoid with a 14-membered macrocycle. The <sup>1</sup>H–<sup>1</sup>H-COSY correlations of H-2 and the olefinic proton at  $\delta_H$  6.26 suggested a double bond ( $\delta_C$  143.8 and 137.8) was located between C-3 and C-4. Both of H-3 and H<sub>3</sub>-18 showed HMBC correlations to the carbonyl unit indicated that C-5 was oxygenated as a carbonyl group. Furthermore, the olefinic proton at  $\delta_H$  6.63 presented <sup>1</sup>H–<sup>1</sup>H-COSY correlations with  $\delta_H$  6.42 and HMBC correlations with C-5 which suggested a disubstituted double bond was posited at C-6 and C-7. The double bond of  $\Delta^{11(12)}$  was determined by the HMBC cross peaks from H<sub>3</sub>-20 to  $\delta_C$  119.8 (C-11) and 138.3 (C-12). An oxygenated quaternary carbon and an oxygenated methine were deduced as C-8 ( $\delta_C$  75.4) and C-9 ( $\delta_C$  78.7) respectively via the HMBC correlations of H-6/C-8 and H<sub>3</sub>-19/C-9.  $\Delta^{3(4)}$ ,  $\Delta^{6(7)}$ , and  $\Delta^{11(12)}$  were all

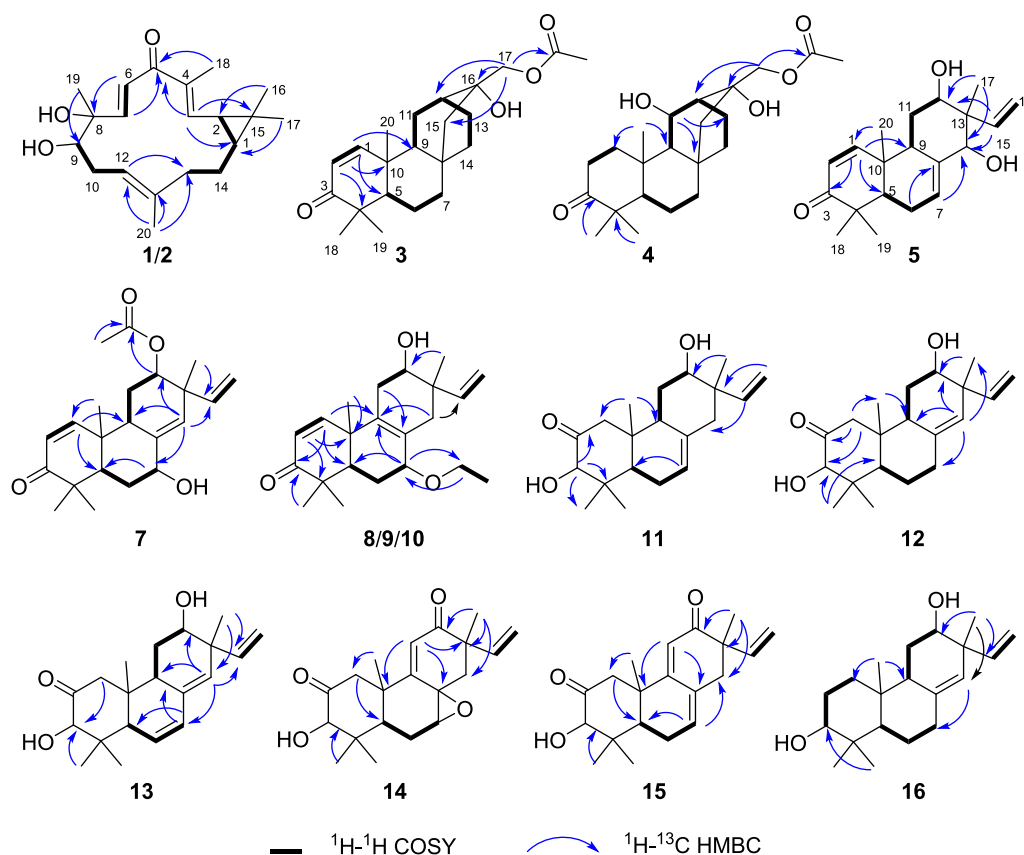


Fig. 2. The key 2D NMR of compounds 1–5 and 7–16.

*E* geometry according to the  $\delta_C$  values of CH<sub>3</sub>-18/CH<sub>3</sub>-20 (<20 ppm) and the *J* values of H-6/H-7 (>16 Hz) (Li et al., 2010). The junction of the two rings between C-1 and C-2 was suggested to be *cis* on the basis of <sup>13</sup>C NMR chemical shifts of C-16 ( $\delta_C$  29.0) and C-17 ( $\delta_C$  16.1), analogously with previous *cis*-fused casbane diterpenoids (Zhang et al., 2005; Li et al., 2010). Two hydroxyls were located at the same side verified by the ROESY correlations of H<sub>3</sub>-19 and H-9 (Fig. 3). Furthermore, the similarity Cotton effect of the experimental electronic circular dichroism (ECD) spectrum of compound 1 between the calculated ECD spectrum of compounds 1a (1,2-*cis*-8 $\alpha$ ,9 $\alpha$ -dihydroxyl) (Fig. 4) established compound 1 as (1*S*,2*R*,8*R*,9*S*)-8,9-dihydroxyl-casbane-3,6,11-triene-5-one and named as jolkiniol A.

The molecular formula of compound 2 was C<sub>20</sub>H<sub>30</sub>O<sub>3</sub> according to the (–)-HR-ESI-MS at *m/z* 353.1884 ([M + Cl]<sup>–</sup> calcd. 353.1889). The NMR data of 2 were similar with those of 1 except for the chemical shifts of C-1 ( $\delta_C$  38.0), C-2 ( $\delta_C$  32.2), C-16 ( $\delta_C$  21.8), and C-17 ( $\delta_C$  23.5) (Table 1) which suggested the *trans* configuration of C-1 and C-2 on the basis of *trans*-fused casbane diterpenoids (Li et al., 2010). The two hydroxyls were located at the same side as well by the ROESY correlations of H<sub>3</sub>-19 and H-9 (Fig. 3). 2a (1,2-*trans*-8 $\alpha$ ,9 $\alpha$ -dihydroxyl) presented almost the same calculated ECD spectrum with the experimental ECD spectrum of 2 (Fig. 4). So, compound 2 was identified as (1*R*,2*R*,8*R*,9*S*)-8,9-dihydroxyl-casbane-3,6,11-triene-5-one and named as jolkiniol B.

Compound 3 was white solids whose molecular formula was C<sub>22</sub>H<sub>32</sub>O<sub>4</sub> according to the (+)-HR-ESI-MS at *m/z* 361.2389 ([M + H]<sup>+</sup> calcd. 361.2373). Two olefinic hydrogens at  $\delta_H$  6.92 (1H, d, *J* = 10.1 Hz) and 5.81 (1H, d, *J* = 10.1 Hz) were observed (Table 1) and were determined as a 1,2-disubstituted double bond by their <sup>1</sup>H-<sup>1</sup>H-COSY correlations (Fig. 2). The <sup>1</sup>H NMR spectrum of 3 also afforded four methyl signals at  $\delta_H$  1.08 (3H, s), 1.14 (3H, s), 1.23 (3H, s), and 2.11 (3H, s), and two oxygenated protons at  $\delta_H$  3.97 (1H, d, *J* = 11.4 Hz) and 4.11 (1H, d, *J* = 11.4 Hz). In the <sup>13</sup>C NMR spectrum, 22 carbons were deduced

as four methyls, seven methylenes, five methines, and six quaternary carbons from which two carbonyl units at  $\delta_C$  205.2 and 171.1 were identified. Compared with the known compound, 17-acetoxy-16-hydroxyl-*ent*-atisane-3-one (Awasaki et al., 1987), there was one 1,2-disubstituted double bond in 3. The other NMR data of 3 were similar with those of 17-acetoxy-16-hydroxyl-*ent*-atisane-3-one. The HMBC correlations from  $\delta_H$  6.92 to C-5/C-9 and from  $\delta_H$  5.81 to C-4/C-10 suggested the double bond was located at C-1 and C-2 (Fig. 2). The oxygenated protons displayed HMBC correlations to a carbonyl unit at  $\delta_C$  205.2, an oxygenated quaternary carbon at  $\delta_C$  72.7 (C-16), a methylene at  $\delta_C$  52.0 (C-15), and a methine at  $\delta_C$  32.6 (C-12) which clarified the 17-acetoxy-16-hydroxyl substituent group of 3. Most of the *ent*-atisane-type diterpenoids isolated from *Euphorbia* species were *ent*-atisane diterpenoids on consideration of biosynthetic pathways (Zhao et al., 2014). Besides, the ROESY correlations of H-5/H-9/H<sub>2</sub>-17 were found as well that indicated these H-atoms were all located at  $\beta$  configuration (Fig. 3). Finally, the calculated ECD spectrum of 3 exhibited similar Cotton effects with the experimental ECD spectrum of 3 (Fig. 4). So, compound 3 was identified as (1*R*)-17-acetoxy-16-hydroxyl-*ent*-atisane-1-ene-3-one and named as jolkiniol C.

Compound 4 afforded the chemical formula of C<sub>22</sub>H<sub>34</sub>O<sub>5</sub> based on the (–)-HR-ESI-MS at *m/z* 423.2378 ([M + HCOO]<sup>–</sup> calcd. 423.2388). Compared with the NMR data of 3, an oxygenated methine at  $\delta_C$  66.9 and  $\delta_H$  4.77 (1H, d, 10.3) (Table 1). At the same time, the absence of the 1,2-disubstituted double bond signal was deduced. On the contrary, two methylenes at  $\delta_C$  39.4 and 34.2 were observed and they were conjugated together due to the <sup>1</sup>H-<sup>1</sup>H-COSY correlations of their protons (Fig. 2). The HMBC correlation of H<sub>3</sub>-20 to the methylene at 39.4 was observed as well. So, the two methylenes were C-1 and C-2 respectively. The <sup>1</sup>H-<sup>1</sup>H-COSY correlations from H-9 to  $\delta_H$  4.77 suggested that C-11 was an oxygenated methine. The  $\beta$  configuration of H-11 was determined by the ROESY correlations of H-11/H-9/H-5/H<sub>2</sub>-17 (Fig. 3). The calculated

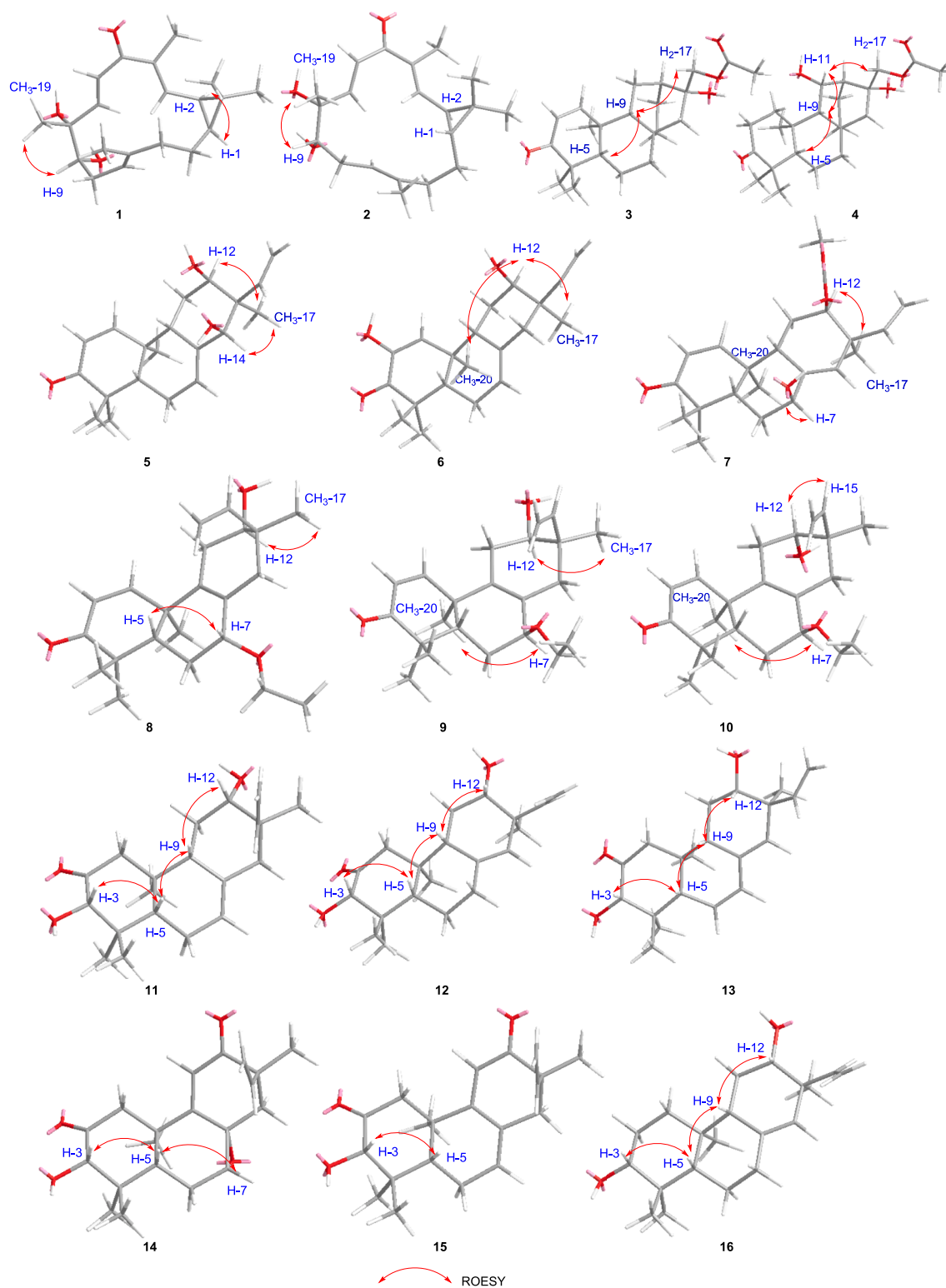


Fig. 3. The ROESY correlations of compounds 1–16.

ECD spectrum of **4** presented similar Cotton effects with the experimental ECD spectrum of **4** (Fig. 4). Thus, **4** was identified as (11*S*,16*R*)-17-acetoxy-11,16-dihydroxy-*ent*-atisane-3-one and named as jolkiniiol D.

According to the (+)-HR-ESI-MS at  $m/z$  317.2112 ( $[M + H]^+$  calcd. 317.2111), compound **5** afforded the chemical formula of  $C_{20}H_{28}O_3$  as white solids. The  $^1H$  NMR spectrum of **5** revealed the signals of four tertiary methyl units at  $\delta_H$  0.88, 1.08, 1.13, and 1.16 (each 3H, s), three

vinyl protons for ABX system at  $\delta_H$  5.29 (1H, d,  $J = 17.8$  Hz), 5.34 (1H, d,  $J = 11.0$  Hz), and 6.30 (1H, dd,  $J = 17.8, 11.0$  Hz), three other vinyl H-atoms at  $\delta_H$  5.88 (1H, br.s), 5.93 (1H, d,  $J = 10.2$  Hz), and 6.92 (1H, d,  $J = 10.2$  Hz), two oxygenated hydrogens at  $\delta_H$  3.98 (1H, br.s) and 3.96 (1H, s) (Table 2). Twenty carbons including four methyls, three methylenes, eight methines, and five quaternary carbons were observed from its NMR spectrum in which a carbonyl unit at  $\delta_C$  204.2, three pairs of double bonds at  $\delta_C$  154.0/142.7/136.8/127.7/125.7/114.4, and two

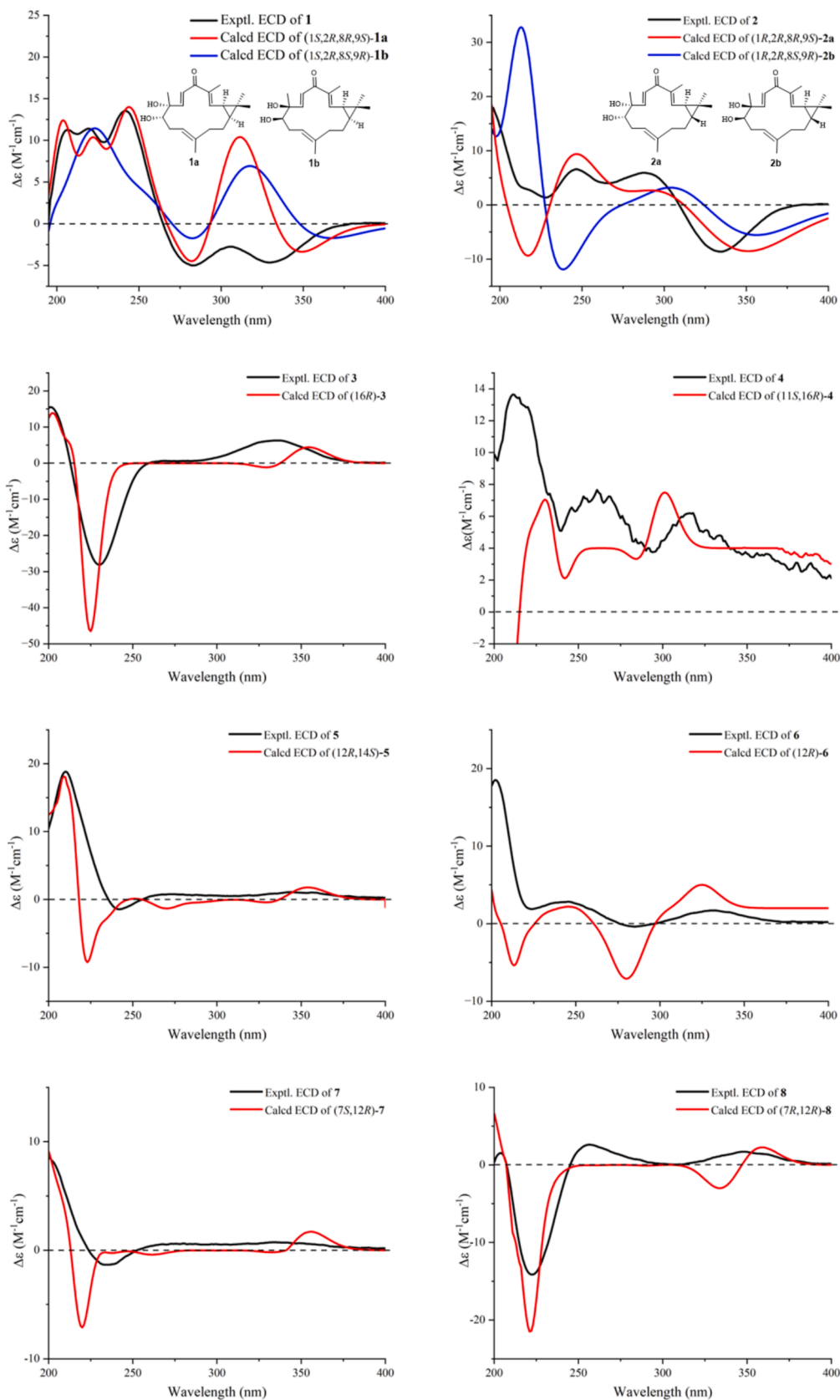


Fig. 4. The ECD calculations of compounds 1–16.

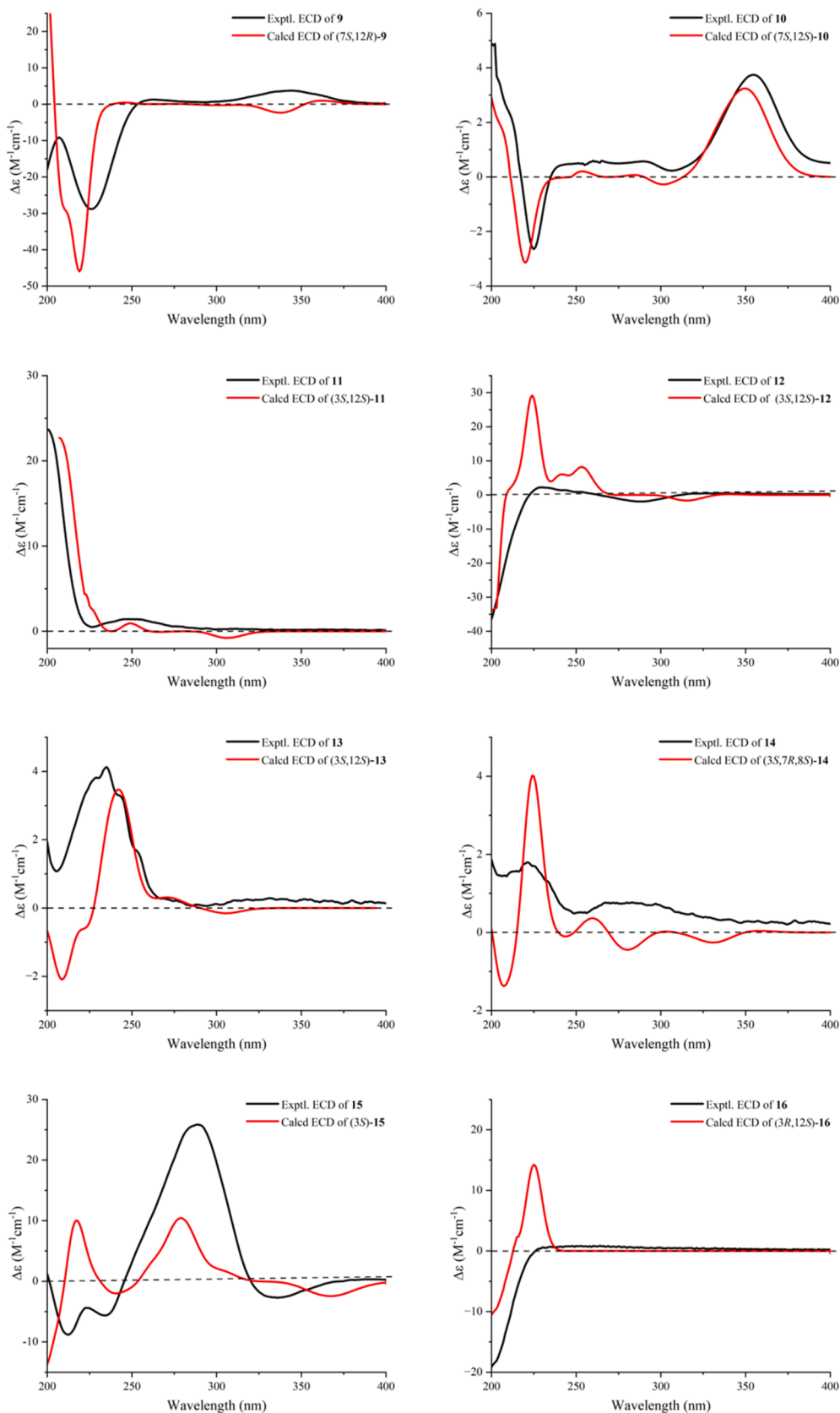


Fig. 4. (continued).

oxygenated C-atoms at  $\delta_C$  81.7 and 74.5 were determined. The detailed analysis of the HSQC,  $^1H$ - $^1H$ -COSY, and HMBC (Fig. 2) spectra allowed the position assignment of all the C-atoms and H-atoms. The NMR data

of **5** were similar to those of 2,12 $\alpha$ -dihydroxyl-*ent*-isopimara-1,7,15-trien-3-one (Tian et al., 2016) except for the olefinic carbon at  $\delta_C$  125.7 (CH,  $\delta_H$  5.93) and the oxygenated C-atom at  $\delta_C$  81.7 (CH,  $\delta_H$  3.96). The

$^1\text{H}$ - $^1\text{H}$  COSY correlation of  $\delta_{\text{H}}$  5.9 and  $\delta_{\text{H}}$  6.92 (H-1) suggested that C-2 was a disubstituted olefinic carbon. H-7 and H-15 showed HMBC correlations to  $\delta_{\text{C}}$  81.7 which positioned C-14 linked with a hydroxyl group. The ROESY correlations of  $\text{CH}_3$ -17 with H-12 and H-14 indicated that these H-atoms were presented on the same side as  $\alpha$ -configuration (Fig. 3). The (+) Cotton effect due to the  $n \rightarrow \pi^*$  transition at 355 nm according to the octant rule for  $\alpha,\beta$ -unsaturated ketones suggested the *trans* junction of A and B rings (Mi et al., 1993). Thus, compound **5** was (12 $\beta$ ,14 $\beta$ )-12,14-dihydroxyl-*ent*-pimara-1,7,15-trien-3-one whose absolute configurations were determined as 12*R*,14*S* by the calculated ECD method (Fig. 4), and named as jolkiniol E.

The (+)-HR-ESI-MS at  $m/z$  317.2115 ( $[\text{M} + \text{H}]^+$  calcd. 317.2111) showed that the molecular formula of **6** was  $\text{C}_{20}\text{H}_{38}\text{O}_3$ . The  $^1\text{H}$  NMR and  $^{13}\text{C}$  NMR data revealed that **6** was an *ent*-isopimara diterpenoid with a carbonyl group, three pairs of double bonds, and two hydroxyl units (Table 2). Huang et al. (Huang et al., 2014) and Tian et al. (Tian et al., 2016) reported almost the same NMR data of two compounds which were similar with those of **6**. The former was identified as 2,12 $\alpha$ -dihydroxy-*ent*-isopimara-1,7,15-trien-3-one and the later was identified as 2,12 $\beta$ -dihydroxy-isopimara-1,7,15-trien-3-one. However, H-12 was not exhibited ROESY correlations with H-5 and H-9 which verified the  $\alpha$ -configuration of H-12 (Fig. 3). The ROESY correlations of H-12 to  $\text{CH}_3$ -20 and  $\text{CH}_3$ -17 also deduced the  $\alpha$ -configuration of H-12. So, the hydroxyl group posited at C-12 was  $\beta$ -configuration. The *trans* junction of A and B rings was determined by the (+) Cotton effect at 355 nm according to the octant rule for  $\alpha,\beta$ -unsaturated ketones (Mi et al., 1993). Compound **6** should be 2,12 $\beta$ -dihydroxy-*ent*-isopimara-1,7,15-trien-3-one and its absolute configurations was determined as 12*R* by comparing the experimental ECD and calculated ECD spectra of **6** (Fig. 4) which was named as jolkiniol F.

Compound **7** was white solids with the molecular formula of  $\text{C}_{22}\text{H}_{30}\text{O}_4$  determined by the (+)-HR-ESI-MS at  $m/z$  359.2208 ( $[\text{M} + \text{H}]^+$  calcd. 359.2217). In the  $^1\text{H}$  NMR spectrum of **7** the most characteristic signals were five tertiary methyl units at  $\delta_{\text{H}}$  1.08, 1.09, 1.15, 1.18 and 2.03 (each 3H, s), three vinyl protons for ABX system at  $\delta_{\text{H}}$  5.00 (1H, d,  $J = 17.4$  Hz), 5.14 (1H, d,  $J = 10.6$  Hz), and 5.82 (1H, dd,  $J = 17.4, 10.6$  Hz), three other vinyl H-atoms at  $\delta_{\text{H}}$  5.60 (1H, s), 5.95 (1H, d,  $J = 10.2$  Hz), and 6.95 (1H, d,  $J = 10.2$  Hz), two oxygenated hydrogens at  $\delta_{\text{H}}$  4.40 (1H, br. s) and 4.88 (1H, dd,  $J = 8.7, 3.4$  Hz) (Table 2). Its  $^{13}\text{C}$  NMR spectrum afforded twenty-two carbons from which two carbonyl units at  $\delta_{\text{C}}$  204.2 and 170.8, three pairs of double bonds at  $\delta_{\text{C}}$  154.9/141.4/138.2/132.4/126.9/115.0, and two oxygenated C-atoms at  $\delta_{\text{C}}$  75.2 and 72.2 were identified. These NMR data were very similar with those of compound **5** except the carbonyl unit at  $\delta_{\text{C}}$  170.8 and a tertiary methyl group at  $\delta_{\text{H}}$  2.03/ $\delta_{\text{C}}$  21.2. They were linked together to form an acetoxy unit according to the HMBC correlation from  $\delta_{\text{H}}$  2.03 to  $\delta_{\text{C}}$  170.8 (Fig. 2). Besides, the oxygenated H-atom at  $\delta_{\text{H}}$  4.88 showed HMBC correlation with  $\delta_{\text{C}}$  170.8 suggested that the acetoxy unit was located at C-12 position. H-5, H<sub>2</sub>-6 and the oxygenated H-atom at  $\delta_{\text{H}}$  4.40 were showed  $^1\text{H}$ - $^1\text{H}$ -COSY correlations together indicated there was a hydroxyl group posited at C-7 position. Both the HMBC correlations from the olefinic proton at  $\delta_{\text{H}}$  5.60 to C-7 and C-12 verified the structure of  $\Delta^{8(14)}$ . The junction of A and B rings was determined as *trans* according to the octant rule for  $\alpha,\beta$ -unsaturated ketones (Mi et al., 1993) as well. The ROESY correlations of  $\text{CH}_3$ -20/H-7 and  $\text{CH}_3$ -17/H-12 showed that H-7 and H-12 were both located at  $\alpha$ -configuration (Fig. 3). Thus, compound **7** was (7 $\beta$ ,12 $\beta$ )-12-acetoxy-7-hydroxyl-*ent*-isopimara-1,8(14),15-trien-3-one whose absolute configurations were determined as 7*S*,12*R* by the calculated ECD spectrum of **7** (Fig. 4) and named as jolkiniol G.

Compounds **8–10** gave the same molecular formula of  $\text{C}_{22}\text{H}_{32}\text{O}_3$  according to the (+)-HR-ESI-MS data. It found five methyl units, three vinyl protons for ABX system, two other vinyl H-atoms, and four oxygenated hydrogens in their  $^1\text{H}$  NMR spectra respectively (Tables 2 and 3). Their  $^{13}\text{C}$  NMR spectra afforded twenty-two carbons including a carbonyl unit, three pairs of double bonds, and three oxygenated C-atoms as well. They gave out an oxygenated methylene at  $\delta_{\text{C}}$  64, a

methyl group at  $\delta_{\text{C}}$  15, and a double bond at 135/128 without vinyl H-atom which were different from those of **5**. The  $^1\text{H}$ - $^1\text{H}$ -COSY correlations from the protons of the oxygenated methylene at  $\delta_{\text{C}}$  64 and the methyl at  $\delta_{\text{C}}$  15 suggested they were linked together to make an ethoxyl group (Fig. 2). HMBC correlations from the H-atoms of the oxygenated methylene to C-7 indicated the ethoxyl group was located at C-7 position. The quaternary carbons of double bond were determined as C-8 and C-9 according to the HMBC correlations of H-7/C-9 and H<sub>2</sub>-11/C-8. Compounds **8–10** exhibited the most same NMR data except the chemical shifts of the oxygenated carbons at C-7 and C-12. For compound **8**, the chemical shifts of C-7 and C-12 were at  $\delta_{\text{C}}$  78.9 and 73.9. For **9**, these were  $\delta_{\text{C}}$  74.8 and 74.4. And, these were  $\delta_{\text{C}}$  74.6 and 72.0 for **10**. We speculated that the configurations of C-7 and C-12 in compounds **8–10** were different. They all showed (+) Cotton effect at 350 nm which suggested the *trans* junction of A and B rings according to the octant rule for  $\alpha,\beta$ -unsaturated ketones (Mi et al., 1993). The observed ROESY correlations of H-5/H-7 and H-12/ $\text{CH}_3$ -17 in **8**, H-7/ $\text{CH}_3$ -20 and H-12/ $\text{CH}_3$ -17 in **9**, and H-7/ $\text{CH}_3$ -20 and H-12/H-15 in **10** indicated that the configurations of **8–10** were 7 $\alpha$ -ethoxy-12 $\beta$ -hydroxyl, 7 $\beta$ -ethoxy-12 $\beta$ -hydroxyl, and 7 $\beta$ -ethoxy-12 $\alpha$ -hydroxyl respectively (Fig. 3). Finally, their absolute configurations were determined according to their experimental ECD and calculated ECD spectra (Fig. 4). So, their structures were identified as shown in Fig. 1 and named as jolkiniols H-J.

Compound **11** assigned the molecular formula of  $\text{C}_{20}\text{H}_{30}\text{O}_3$  on the basis of (+)-HR-ESI-MS  $[\text{M} + \text{H}]^+$  at  $m/z$  319.2270 ( $[\text{M} + \text{H}]^+$  calcd. 319.2268). Its  $^1\text{H}$  NMR spectrum afforded three vinyl protons for ABX system, one other vinyl H-atom, four methyl units, and two oxygenated H-atoms (Table 3). Its  $^{13}\text{C}$  NMR data gave twenty carbons including a carbonyl unit, two pairs of double bonds, and two oxygenated C-atoms. Just as that of compound **10**, the ABX system was formed by H-15 and H<sub>2</sub>-16. C-12 was ascribed to link with a hydroxy group by the HMBC correlations from  $\text{CH}_3$ -17 to the oxygenated C-atom at  $\delta_{\text{C}}$  73.7 (Fig. 2). The  $^1\text{H}$ - $^1\text{H}$ -COSY correlations of H-9/H<sub>2</sub>-11/H-12 verified C(12)-hydroxyl as well. Furthermore,  $^1\text{H}$ - $^1\text{H}$ -COSY cross peaks of H-5/H<sub>2</sub>-6/H-7 suggested that H-7 was a vinyl H-atom. The other oxygenated C-atom at C-3 position assigned by the HMBC correlation from  $\text{CH}_3$ -18 to C-3. H-3 presented HMBC correlation to the carbonyl unit which determined C-2 as a carbonyl C-atom. Both of the configurations of the hydroxyl groups at C-3 and C-12 positions were  $\alpha$ -oriented according to the ROESY cross peaks of H-3/H-5/H-9/H-12 (Fig. 3). The calculated ECD spectrum of **11** was well matched with the experimental ECD spectrum of **11** (Fig. 4). Thus, **11** was identified as (3*S*,12*S*)-3,12-dihydroxyl-*ent*-isopimara-7,15-dien-2-one and named as jolkiniol K.

Compound **12** afforded almost the same HR-ESI-MS and NMR data as those of **11**. The difference between their NMR data was a double bond. For **11**, the chemical shifts were at  $\delta_{\text{C}}$  133.2 and 122.3. For **12**, the chemical shifts were at  $\delta_{\text{C}}$  136.3 and 128.6. The  $\Delta^{8(14)}$  was established by the HMBC correlations from the olefinic H-atom at  $\delta_{\text{H}}$  5.12 to C-7, C-9, C-12, and C-17 (Fig. 2). The ROESY cross peaks of H-3/H-5/H-9/H-12 were observed as well which illuminated the  $\alpha$ -oriented hydroxyl groups at C-3 and C-12 positions (Fig. 3). The structure of **12** was (3*S*,12*S*)-3,12-dihydroxyl-*ent*-isopimara-8(14),15-dien-2-one based on the calculated ECD spectrum of **12** (Fig. 4) and named as jolkiniol L.

Compound **13** presented the molecular formula  $\text{C}_{20}\text{H}_{28}\text{O}_3$ , 2 mass units lower than that of **12**, by (+)-HR-ESI-MS at  $m/z$  339.1932 ( $[\text{M} + \text{Na}]^+$  calcd. 339.1931). Interpretation of the NMR spectrum established the *ent*-isopimara skeleton of **13** being identical with that of **12**, except that there was a double bond in **13** at  $\delta_{\text{H}}$  6.12/5.68 and  $\delta_{\text{C}}$  130.7/126.1 (Table 4). The  $^1\text{H}$ - $^1\text{H}$ -COSY correlations of H-5/ $\delta_{\text{H}}$  6.12/5.68 indicated that the double bond was located at C-6 and C-7 positions (Fig. 2). This hypothesis was also corroborated by the observations of HMBC associations of H-7/C-5, H-7/C-9, H-14/C-7. The carbonyl unit, hydroxy groups, and the other two double bonds of **13** were same as those of **12** based on its 2D NMR data. The  $\alpha$ -oriented hydroxyl groups at C-3 and C-12 positions were assigned by the ROESY correlations of H-3/H-5/H-9/H-12 (Fig. 3). And then, the absolute configurations of **13** were deduced

as 3*S*,12*S* by the same Cotton effects of the calculated ECD spectrum of **13** and the experimental ECD spectrum of **13** (Fig. 4). So, **13** was (3*S*,12*S*)-3,12-dihydroxyl-*ent*-isopimara-6,8(14),15-trien-2-one and named as jolkiniol M.

Compound **14** displayed the molecular formula of C<sub>20</sub>H<sub>26</sub>O<sub>4</sub> as derived from the (+)-HR-ESI-MS at *m/z* 331.1915 ([M + H]<sup>+</sup> calcd. 331.1904). The <sup>1</sup>H NMR spectrum of **14** displayed the characteristic resonances for three vinyl protons for ABX system, one other vinyl H-atom at δ<sub>H</sub> 5.93 (1H, s), four methyl units, and two oxygenated H-atoms at δ<sub>H</sub> 3.91 (1H, d, *J* = 6.0 Hz) and 3.47 (1H, s) (Table 4). Two carbonyl units at δ<sub>C</sub> 208.8 and 202.1, two pairs of double bonds, and three oxygenated C-atoms at δ<sub>C</sub> 81.9/60.1/54.9 were observed in the <sup>13</sup>C NMR spectrum of **14**. The oxygenated C-atoms were divided into two methines and one quaternary carbon. C(2)-carbonyl group and C(3)-hydroxyl unit were established by the interpretation of the 2D NMR spectra as those of **11** (Fig. 2). Except for the vinyl protons for ABX system, the other vinyl H-atom at δ<sub>H</sub> 5.93 was displayed HMBC correlations to C-10 and C-13 suggested that this double bond was located between C-9 and C-11. Besides, C-8 was illuminated as an oxygenated quaternary C-atom on the basis of the HMBC correlation of H-11 and the oxygenated quaternary carbon at δ<sub>C</sub> 54.9. The other oxygenated C-atom was C-7 according to the <sup>1</sup>H-<sup>1</sup>H-COSY cross peaks of H-5/H<sub>2</sub>-6/H-7. C-12 was a carbonyl unit assigned by the HMBC correlations from CH<sub>3</sub>-17 to the carbonyl C-atom at δ<sub>C</sub> 202.1. Thus, the remaining one unsaturation degree required by the molecular formula of **14** was attributed to one ring that might be located as C-7 and C-8 to form an epoxy ring. The configurations of H-3 and H-7 were β-oriented according to the ROESY cross peaks of H-3/H-5/H-7 (Fig. 3). The calculated ECD spectrum of **14** (Fig. 4) determined its absolute configurations were 3*S*,7*R*,8*S*. Thus, **14** was (3*S*,7*R*,8*S*)-7,8-epoxy-3-hydroxy-*ent*-isopimara-9(11),15-dien-2,12-dione and named as jolkiniol N.

Compound **15** gave out the molecular formula of C<sub>20</sub>H<sub>26</sub>O<sub>3</sub> which came from the (+)-HR-ESI-MS at *m/z* 315.1960 ([M + H]<sup>+</sup> calcd. 315.1955). Compared with the NMR data of **14**, the absence of the epoxy ring signals and the presence of one double bond at δ<sub>C</sub> 130.8 and 129.4 were observed (Table 4). The <sup>1</sup>H-<sup>1</sup>H-COSY correlations of H-5/H<sub>2</sub>-6/H-atom at δ<sub>H</sub> 6.11 deduced the double bond was located between C-7 and C-8 positions which was determined by the HMBC correlations from H-7 to C-5 and C-14 as well (Fig. 2). The other NMR signals were similar with those of **14**. H-3 was β-oriented according to the ROESY cross peaks of H-3/H-5 (Fig. 3). Thus, the absolute configuration of **15** was 3*S* based on the comparison of the calculated ECD spectrum of **15** and experimental ECD spectrum of **15** (Fig. 4). Finally, compound **15** was identified as (3*S*)-3-hydroxy-*ent*-isopimara-7,9(11),15-trien-2,12-dione and named as jolkiniol O.

Compound **16** assigned the molecular formula of C<sub>20</sub>H<sub>30</sub>O<sub>2</sub> based on the (+)-HR-ESI-MS [M + H]<sup>+</sup> at *m/z* 305.2462 ([M + H]<sup>+</sup> calcd. 305.2475). Just as those of compound **12**, three vinyl protons for ABX system, one other vinyl H-atom, four methyl units, and two oxygenated H-atoms were found in its <sup>1</sup>H NMR spectrum (Table 4). Its <sup>13</sup>C NMR data gave twenty carbons including two pairs of double bonds, and two oxygenated C-atoms. The ABX system was formed by H-15 and H<sub>2</sub>-16 undoubtedly. The hydroxy group at C-12 position and Δ<sup>8(14)</sup> were deduced by the HMBC correlations from CH<sub>3</sub>-17 to the oxygenated C-atom at δ<sub>C</sub> 72.8 and to the olefinic C-atom at δ<sub>C</sub> 124.6 (Fig. 2). Furthermore, <sup>1</sup>H-<sup>1</sup>H-COSY cross peaks of H-1/H-2/the oxygenated at δ<sub>H</sub> 3.26 and the HMBC correlation from CH<sub>3</sub>-19 to the oxygenated C-atom at δ<sub>C</sub> 79.0 indicated that C-3 was an oxygenated C-atom. H-3 and H-12 were both β-oriented according to the ROESY cross peaks of H-3/H-5/H-9/H-12 (Fig. 3). The calculated ECD spectrum of **16** was well matched with the experimental ECD spectrum of **16** (Fig. 4). Therefore, **16** was identified as (3*R*,12*S*)-3,12-dihydroxyl-*ent*-isopimara-7,15-dien and named as jolkiniol P.

### 3.2. Cytotoxicity on pancreatic cancer SW1990 cells

Compounds **1–16** were evaluated the cytotoxicity on pancreatic cancer SW1990 cells using CCK-8 method *in vitro* and paclitaxel was used as the positive control. The results showed that **1** and **9** displayed obvious cytotoxicity with the IC<sub>50</sub> values 26.50 ± 6.36 μM and 21.09 ± 5.98 μM respectively which were stronger than that of paclitaxel (IC<sub>50</sub> = 45.01 ± 7.65 μM) (Table 5). Other compounds did not present cytotoxicity on pancreatic cancer SW1990 cells with the IC<sub>50</sub> values > 50 μM.

### 3.3. Flow cytometric results

FITC Annexin-V combined with PI were used to detect the effects of compounds **1** and **9** on the apoptosis cycle of tumor cells. The experiments showed that the percentages of SW1990 cells in pre apoptosis cycle were increased with dose dependent after the administration of compounds **1** and **9** (Fig. 5). It suggested us that **1** and **9** could promote the pre-apoptosis of SW1990 cells to act a role in anti-tumor.

### 3.4. Western blot assay results

Bcl-2 is an inhibitor of apoptosis in mitochondria, and Bax is a pro-apoptotic protein. Bcl-2 forms a heterodimer with the Bax and inhibits the pro-apoptotic activity of Bax to maintain the integrity of the mitochondrial outer membrane and block mitochondrial apoptosis (Hu et al., 2015; Zhang et al., 2018). Caspase-3 is an aspartate-specific protease with the ability of breaking down proteins which is recognized as an apoptosis executor as well (Hu et al., 2015; Zhang et al., 2018). Therefore, we investigated the levels of Bcl-2, Bax, and Caspase-3 proteins in pancreatic cancer SW1990 cells after the treatment of compounds **1** and **9**. As a result, compound **1** could down-regulate the expressions of Bcl-2 and up-regulate the expressions of Bax and Caspase-3. The protein levels of Bcl-2 in SW1990 cells were decreased significantly with the administration of compound **9**. But compound **9** only up-regulated the expressions of Bax and not affected the protein levels of Caspase-3 (Fig. 6). It reminded that compounds **1** and **9** played a role in inhibiting tumor cells by decreasing the expressions of intracellular anti-apoptotic protein Bcl-2 and increasing the levels of apoptotic proteins Bax and Caspase-3.

### 3.5. Molecular docking results and druggability prediction

The above findings suggested that Bcl-2 played an important role in the anti-tumor process of compounds **1** and **9**. To reveal their binding sites with Bcl-2, we subjected **1** and **9** to molecular docking with Bcl-2 (Fig. 7). It found that compound **1** was able to inhibit Bcl-2 with the binding energy of -6.2 kcal/mol by forming hydrogen bonds with aspartic acid (ASP), arginine (ARG), and asparagine (ASN) residues of Bcl-2 whose bond lengths were 3.0, 3.1, 2.6, and 2.3, respectively. Compound **9** also showed a good free energy binding ability with Bcl-2

**Table 5**  
Cytotoxicity of compounds **1–16** against human pancreatic cancer SW1990 cells.

Compounds	IC <sub>50</sub> (μM) <sup>a</sup>	Compounds	IC <sub>50</sub> (μM) <sup>a</sup>
<b>1</b>	26.50 ± 6.36	<b>9</b>	21.09 ± 5.98
<b>2</b>	>50	<b>10</b>	>50
<b>3</b>	>50	<b>11</b>	>50
<b>4</b>	>50	<b>12</b>	>50
<b>5</b>	>50	<b>13</b>	>50
<b>6</b>	>50	<b>14</b>	>50
<b>7</b>	>50	<b>15</b>	>50
<b>8</b>	>50	<b>16</b>	>50
Paclitaxel <sup>b</sup>	45.01 ± 7.65		

<sup>a</sup> Data were expressed as means ± SD (n = 3).

<sup>b</sup> Paclitaxel was used as a positive control.

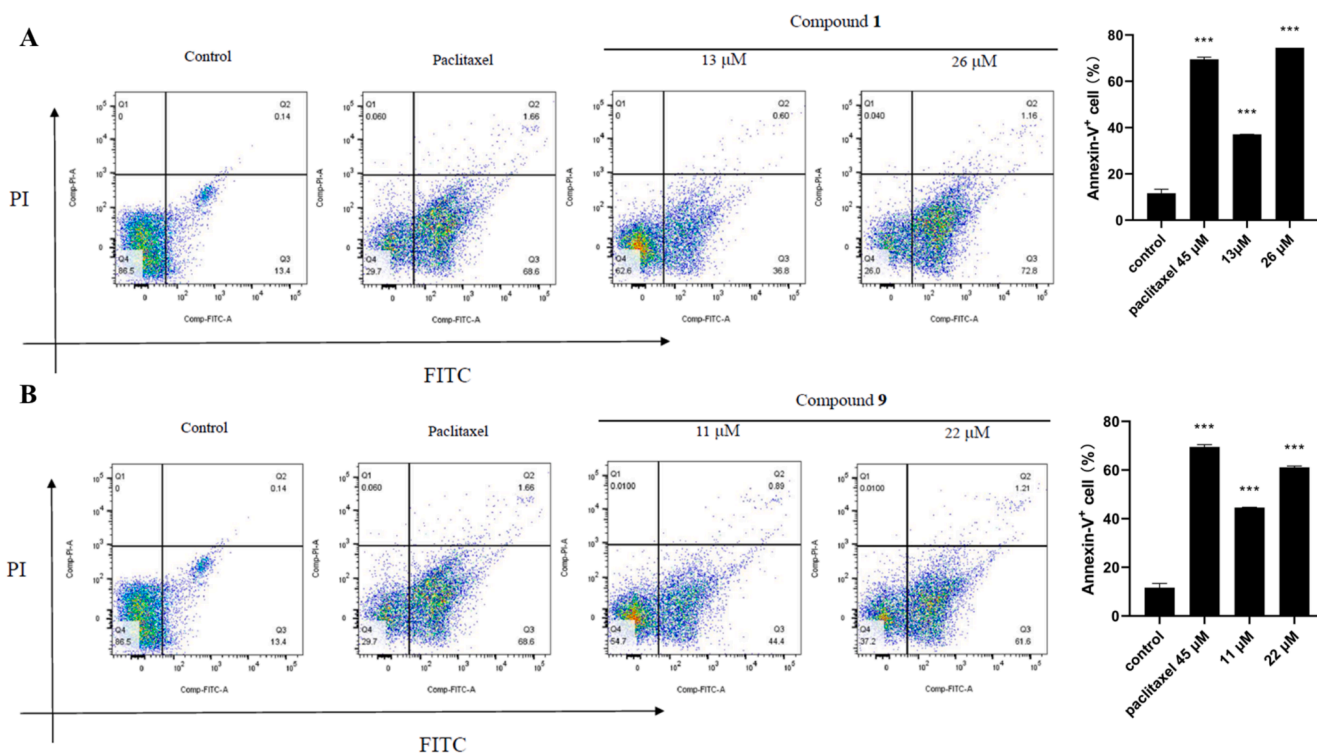


Fig. 5. Compounds 1 (A) and 9 (B) induced the apoptosis rates of pancreatic cancer SW1990 cells (means  $\pm$  SEM,  $n = 3$ ; \*\*\* $P < 0.001$  vs control (DMSO)).

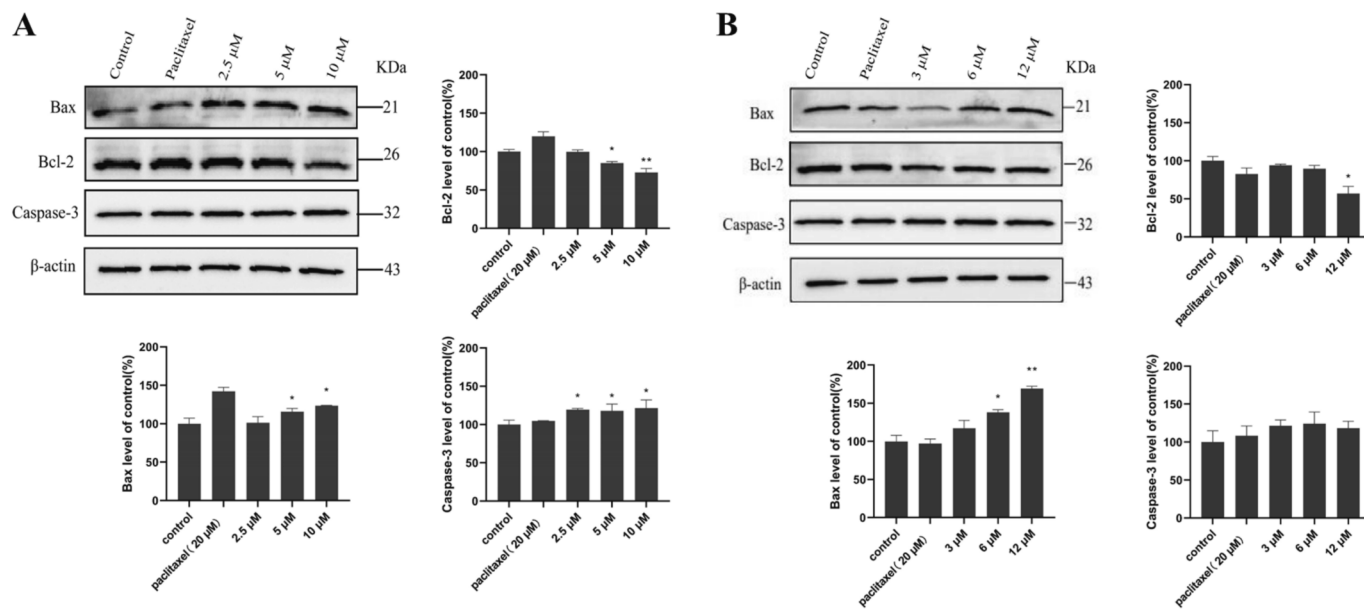


Fig. 6. The effects of compounds 1 (A) and 9 (B) on Bcl-2, Bax, and Caspase-3 proteins in pancreatic cancer SW1990 cells (means  $\pm$  SEM,  $n = 3$ ; \* $P < 0.05$ , \*\* $P < 0.01$  vs control (DMSO)).

with the molecular docking binding energy of  $-5.4$  kcal/mol and formed hydrogen bonds with ASP, ARG, glutamic acid (GLU), and lysine acid (LYS) residues with the bond lengths of 2.3, 2.9, 2.2, 3.5, and 2.3, respectively (Table 6).

The druggability prediction showed that compounds 1 and 9 were lipophilic molecules with low solubility, low molecular polar surface area, and high Log P values. Thus, they were easily absorbed through the digestive system and displayed high plasma protein binding rates and blood-brain barrier permeabilities. Besides, the predictions also suggested that 1 and 9 could not inhibit the CYP2D6 to generated

hepatotoxicity (Table 6). These results provided the basis for the later experimental study of their drug properties.

The spread of *E. jolkinii* caused serious damages to alpine meadows that prompted the research of *E. jolkinii* on bioactive compounds and allelochemicals (Huang et al., 2014; He et al., 2008; Duan et al., 2024; Niu et al., 2024). In this paper, we investigated the anti-tumor effects of diterpenoids from *E. jolkinii* roots that was helpful for the utilization of *E. jolkinii* and the development of anti-pancreatic cancer drugs. However, the allelochemicals of *E. jolkinii* were unclear and the prevention of *E. jolkinii* has not been solved yet. Diterpenoids, as the characteristic

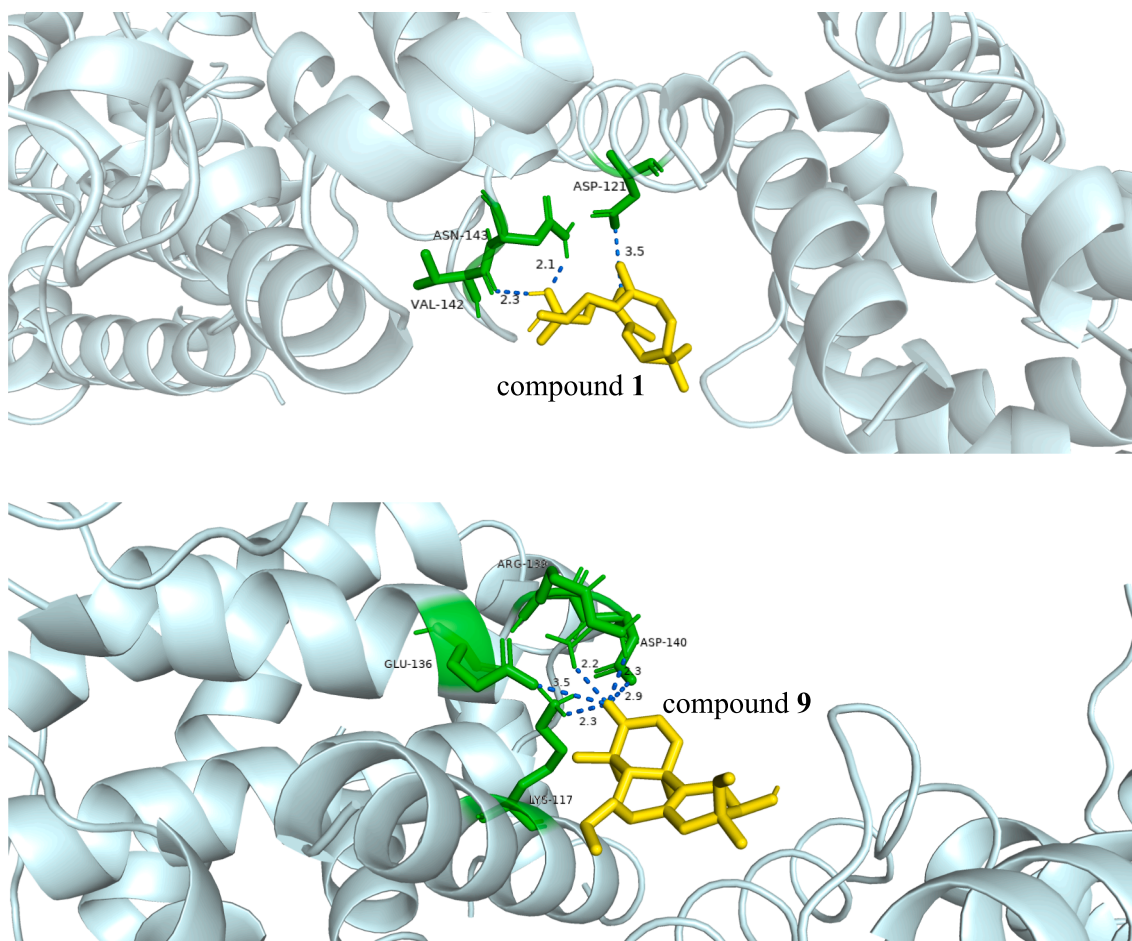


Fig. 7. The molecular docking results of 1 and 9 with Bcl-2 protein.

**Table 6**  
The molecular docking and the druggability prediction of compounds 1 and 9.

Properties	1	9
Binding energy (kcal/mol)	-6.2	-5.4
Interaction residues	ASP-121, ASN-143, VAL-142	ASP-140, ARG-139, GLU-136, LYS-117
Solubility	2	2
Log of the octanol–water partition coefficient (Log P)	3.635	3.487
Molecular polar surface area (FPSA)	0.154	0.117
Absorption	0	0
Blood brain barrier (BBB)	1	1
Plasma protein binding (PPB)	true	true
CYP2D6	false	false
Hepatotoxicity	false	false

compounds isolated from *E. jolkini*, they might present ecological significance, such as allelopathy or antifeedant activity. Therefore, we plant design experiments to study the allelopathy of these diterpenoids to reveal the allelochemicals of *E. jolkini* in the future which will help to control *E. jolkini* and protect the alpine meadow ecosystem.

#### 4. Conclusions

In this study, sixteen new diterpenoids were isolated from *E. jolkini* roots including casbane, *ent*-atisane, and *ent*-isopimarane types. Compounds 1 and 9 exhibited obvious cytotoxicity on pancreatic cancer SW1990 cells with the IC<sub>50</sub> values of 26.50 ± 6.36 and 21.09 ± 5.98 μM respectively. Mechanism study indicated that 1 and 9 could promote the

pre-apoptosis of SW1990 cells and regulate the expressions of Bcl-2, Bax, and Caspase-3 proteins to play anti-tumor role. Molecular docking results showed that both of 1 and 9 displayed strong bond abilities with Bcl-2 protein and possessed good druggabilities. This study suggested that *E. jolkini* roots contained diverse diterpenoids with cytotoxicity on pancreatic cancer SW1990 cells by regulating the expressions of Bcl-2, Bax, and Caspase-3 proteins which promoted the preventions and utilizations of *E. jolkini* in subalpine meadows of southwest China.

#### Author agreement

The manuscript is approved by all authors for publication. I would like to declare on behalf of my co-authors that the work described was original research that has not been published previously, and not under consideration for publication elsewhere, in whole or in part. All the authors listed have approved the manuscript that is enclosed.

#### CRediT authorship contribution statement

**Xinglong Chen:** Writing – review & editing, Writing – original draft, Formal analysis, Data curation. **Hongbo Zhu:** Methodology, Investigation. **Haiying Zhang:** Investigation. **Tang Zhou:** Investigation, Conceptualization. **Xingxi Li:** Investigation. **Bo Hou:** Investigation. **Weiyang Hu:** Writing – review & editing, Supervision. **Rongping Zhang:** Writing – review & editing, Visualization.

#### Declaration of competing interest

The authors declare that they have no known competing financial

interests or personal relationships that could have appeared to influence the work reported in this paper.

## Acknowledgments

This study was financed by the Applied Basic Research Programs of Yunnan Province (No. 202201AU070166), the National Natural Science Foundation of China (No. 32160107), the Program of Yunling Scholarship (YNWR-YLXZ-2019-019), the Social Development Special Projects-Key Research and Development Plan of Science and Technology Department of Yunnan Province (No. 202303AC100025).

## Appendix A. Supplementary material

1D and 2D NMR, HRESIMS, UV, and IR spectra of compounds 1–16 can be found Supplementary material. The manuscript is approved by all authors for publication. I would like to declare on behalf of my co-authors that the work described was original research that has not been published previously, and not under consideration for publication elsewhere, in whole or in part. All the authors listed have approved the manuscript that is enclosed. Supplementary data to this article can be found online at <https://doi.org/10.1016/j.arabjc.2024.106012>.

## References

- Aamazadeh, F., Ostadrahimi, A., Rahbar, S.Y., Barar, J., 2020. Bitter apricot ethanolic extract induces apoptosis through increasing expression of Bax/Bcl-2 ratio and caspase-3 in PANC-1 pancreatic cancer cells. *Mol. Biol. Rep.* 47, 1895–1904.
- Awasaki, T., Wahara, K., Oda, N., 1987. Isolation and characterization of 3-oxoatisane-16 $\alpha$ ,17-diol from *Euphorbia acaulis*. *J. Nat. Prod.* 50, 790–793.
- Chen, X.L., Geng, Y.J., Li, F., Hu, W.Y., Zhang, R.P., 2022. Cytotoxic terpenoids from *Tripterygium hypoglaucum* against human pancreatic cancer cells SW1990 by increasing the expression of Bax protein. *J. Ethnopharmacol.* 289, 115010.
- Duan, R., Luo, Q., Xiao, X., Niu, Q.M., Liu, Y., Gui, B.L., Zhong, L.Q., Chu, X.H., Shan, G. L., 2024. Analysis of secondary metabolites and study on allelopathic effects of main substances of *Euphorbia jolkini*. *Acta Agr. Sin.*
- Feng, A.Q., Li, Y.Z., Gao, J.B., Wu, S.H., Feng, A.X., 2017. The determinants of stream flow variability and variation in Three-River Source of China: climate change or ecological restoration? *Environ. Earth Sci.* 76, 696.
- Garg, S.K., Chari, S.T., 2020. Early detection of pancreatic cancer. *Curr. Opin. Gastroen.* 36, 456–461.
- Guo, L.Z., Li, J.H., He, W., Liu, L., Huang, D., Wang, K., 2019. High nutrient uptake efficiency and high water use efficiency facilitate the spread of *Stellera chamaejasme* L. in degraded grasslands. *BMC Ecol.* 19 (2), 270–275.
- Gupta, S., Harper, A., Ruan, Y.B., Barr, R., Frazier, A.L., Ferlay, J., Steliarova-Foucher, E., Fidler-Benaoudia, M.M., 2020. International trends in the incidence of cancer among adolescents and young adults. *J. Natl. Cancer Inst.* 112, 1105–1117.
- He, F., Pu, J.X., Huang, S.X., Xiao, W.L., Yang, L.B., Li, X., Zhao, Y., Ding, J., Xu, C., Sun, H.D., 2008. Eight new diterpenoids from the roots of *Euphorbia nematocypa*. *Helv. Chim. Acta* 91, 2139–2147.
- Hu, W.Y., He, Z.Y., Yang, L.J., Zhang, M., Xiao, Z.C., 2015. The Ca<sup>2+</sup> channel inhibitor 2-APB reverses  $\beta$ -amyloid-induced LTP deficit in hippocampus by blocking BAX and caspase-3 hyperactivation. *Br. J. Pharmacol.* 172, 2273–2285.
- Huang, C.S., Luo, S.H., Li, Y., Li, C.H., Hua, J., Liu, Y., Jing, S.X., Wang, Y., Yang, M.J., Li, S.H., 2014. Antifeedant and antiviral diterpenoids from the fresh roots of *Euphorbia jolkini*. *Nat. Prod. Bioprospect.* 4, 91–100.
- Kunovaky, L., Tesarikova, P., Kala, Z., 2018. The use of biomarkers in early diagnostics of pancreatic cancer. *Can. Gastroen. Hepatol.* 201, 5389820.
- Li, Y., Carbone, M., Vitale, R.M., Amodeo, P., Castelluccio, F., Sicilia, G., Mollo, E., Nappo, M., Cimino, G., Guo, Y.W., Gavagnin, M., 2010. Rare casbane diterpenoids from the hainan soft coral *Sinularia depressa*. *J. Nat. Prod.* 73, 133–138.
- Li, J.Y., Chu, X.H., Yin, H.Y., Mei, W.J., Xie, Y., Shan, G.L., 2021. Response of vegetation succession to enclosure in *Euphorbia jolkini* subalpine meadow. *Chin. J. Grass.* 43, 10–16.
- Liu, W.L., Ho, J.C.K., Qin, G., 2002. Jolkinolide B induced neuroendo-crine differentiation of human prostate LNCaP cancer cell line. *Biochem. Pharmacol.* 63, 951–957.
- Luo, H., Wang, A., 2006. Induction of apoptosis in K562 cells by jolkinolide B. *Can. J. Physiol. Pharm.* 84, 959–965.
- Mi, J.F., Xu, R.S., Yang, Y.P., Yang, P.M., 1993. Studies on circular dichroism of diterpenoids from *Mallotus anomalus* and sesquiterpenoid tussilagone. *Acta Pharm. Sin.* 28, 105–109.
- Neoptolemos, J.P., Kleeff, J., Michl, P., Costello, E., Greenhalf, W., Palmer, D.H., 2018. Therapeutic developments in pancreatic cancer: current and future perspectives. *Nat. Rev. Gastroen. Hepatol.* 15 (6), 333–348.
- Niu, Q.M., Yang, X., Ma, Z.Y., Chu, X.H., Luo, Q., Liu, Y., Xie, Y., Liu, J., Shan, G.L., 2024. Study on the allelopathic effects of extracts from the roots of *Euphorbia jolkini* on three high quality forages. *Chin. J. Grass.* 46, 135–142.
- Siegel, R.L., Miller, K.D., Wagle, N.S., Jemal, A., 2023. Cancer statistics, 2023. *CA: Cancer J. Clin.* 73, 1–112.
- Siegel, R.L., Giaquinto, A.N., Jemal, A., 2024. Cancer statistics, 2024. *CA: Cancer J. Clin.* 74, 1–114.
- State Pharmacopoeia Commission of P.R. China, Pharmacopoeia of P.R. China, 1997. China Medical Science Press, Beijing, 44, 026.
- Tian, R.T., Lu, Y., Chen, D.F., 2016. Four new diterpenoids from the roots of *Euphorbia pekinensis*. *Chem. Biodivers.* 13, 1404–1409.
- Wei, Y., Wang, H.G., Chen, C.B., Wang, C.G., Song, W.Q., Li, D.W., Zhao, L.Q., 2023. Annexin V-FITC/PI detection of apoptosis experiment. *J. Biol.* 40, 119–122.
- Xu, H.Y., Chen, Z.W., Hou, J.C., 2013b. Jolkinolide B induces apoptosis in MCF-7 cells through inhibition of the P13K/Akt/mTOR signaling pathway. *Oncol. Rep.* 29, 212–218.
- Xu, C., Wu, A., Zhu, H., Fang, H., Xu, L., Ye, J., Shen, J., 2013a. Melatonin is involved in the apoptosis and necrosis of pancreatic cancer cell line SW-1990 via modulating of Bcl-2/Bax balance. *Biomed. Pharmacother.* 67, 133–139.
- Yang, J.H., Bai, T.C., Shi, L.L., Hou, B., Tang, R., Zhang, R.P., Chen, X.L., 2023. Antihyperlipidemic effect of *Vaccinium dunalianum* buds based on biological activity screening and LC-MS. *J. Ethnopharmacol.* 289, 115010.
- Yang, Y., Wang, J., Chen, Y., Cheng, F., He, Z., 2019. Remote-sensing monitoring of grassland degradation based on the GDI in Shangri-La, China. *Remote Sens.* 11 (24), 3030.
- Zhang, Y.W., Li, Z.M., Min, Q.X., Palida, A., Zhang, Y.Y., Tang, R.T., Chen, L.X., Li, H., 2018. 8-chrysoeriol, as a potential Bcl-2 inhibitor triggers apoptosis of SW1990 pancreatic cancer cells. *Bioorg. Chem.* 77, 478–484.
- Zhang, C.X., Yan, S.J., Zhang, G.W., Lu, W.G., Su, J.Y., Zeng, L.M., Gu, L.Q., Yang, X.P., Lian, Y.J., 2005. Cytotoxic diterpenoids from the soft coral *Sinularia microclavata*. *J. Nat. Prod.* 68, 1087–1089.
- Zhao, J.X., Liu, C.P., Qi, W.Y., Han, M.L., Han, Y.S., Wainberg, M.A., Yue, J.M., 2014. Eurifoloids A-R, structurally diverse diterpenoids from *Euphorbia nerifolia*. *J. Nat. Prod.* 77, 2224–2233.
- Zhao, Y.H., Memmott, J., Vaughan, I.P., Li, H.D., Ren, Z.X., Lázaro, A., Zhou, W., Wang, J.W., Liang, H., Li, D.Z., Wang, H.T., 2012. The impact of a native dominant plant, *Euphorbia jolkini*, on plant-flower visitor networks and pollen deposition on stigmas of co-flowering species in sub-alpine meadows of Shangri-La, SW Chin. *J. Ecol.* 109, 2107–2120.
- Zhong, D.C., Chen, C., Li, T., 2020. Study on the Caspase 3/Bax/Bcl-2 signal pathway mechanism of induction apoptosis effect of piperine in human pancreatic cancer PANC-1 Cell. *Chin. J. Mod. App. Pharm.* 37, 1687–1691.